Study on the LQR Control of High-speed Elevator Car Horizontal Vibration Based on the Jumping Inertia Weight Particle Swarm Optimization

Qin He, Hua Li and Ruijun Zhang

School of Mechanical and Electrical Engineering, Shandong Jianzhu University, Jinan 250101, China.
E-mail: heqin67271@163.com

Tichang Jia

School of Mechanical Engineering and Automation, Northeastern University, Shenyang 110819, China.

(Received 10 November 2021; accepted 28 March 2022)

To reduce the horizontal vibration of a high-speed elevator car caused by the excitation of a guide rail more effectively, a differential magnetic suspension active guide shoe based on the principle of the differential magnetic suspension actuator is designed. Then the dynamic model of the active vibration damping system of the elevator car is established and an LQR controller is designed to reduce the horizontal vibration of the car. To search the weighting coefficient matrix of the LQR controller more efficiently, an algorithm named Jumping inertia Weight Particle Swarm Optimization (JWPSO) algorithm is proposed, and the frequently used fitness function verifies the optimization effect of the JWPSO algorithm. The weighting coefficient matrix of the LQR controller is optimized using the JWPSO algorithm. Finally, the impact of the JWPSO algorithm-optimized LQR controller is verified by MATLAB. The simulation result shows that the designed active vibration controller can effectively attenuate the horizontal vibration of the elevator car, and the control effect is significantly better than the LQR controller optimized by the GA algorithm and the H∞ controller optimized by LMI. This paper provided a new method for horizontal vibration reduction of the high-speed elevator car.

1. INTRODUCTION

With the rapid development of urbanization, high-rise and super high-rise buildings have become mainstream in urban construction. The number of high-rise and super high-rise buildings is increasing and so are the operating speeds of elevators. When the elevator is running at high speed, the elevator car will produce violent horizontal vibration under various comprehensive factors. One of the main factors for the horizontal vibration of the car is that the elevator guide mechanism is excited by the external excitation,[1,2] and the guide excitation is mainly caused by the unevenness of the guide rail and the installation error.[3–5]

The horizontal vibration of high-speed elevator cars will affect the comfort of passengers and reduce the service life of precision instruments on the elevator. To reduce the vibration of the elevator car better, the research on the vibration active control of elevator lifting systems[6–9] has become the primary direction of relevant research. At present, the main way to reduce the horizontal vibration is using the active guide shoe equipped with either a hydraulic actuator or electromagnetic actuator to offset the horizontal vibration of the car. However, the cylinder of the hydraulic actuator has friction resistance. The response speed of the hydraulic active guide shoe will be affected by the frictional force when excited. It is inconvenient that the electromagnetic actuators output control force in two directions to the elevator car. Therefore, in this paper, a differential magnetic levitation active guide shoe is designed based on the principle of a magnetic levitation system,[10–13] which has the advantages of no contact, no friction, fast response[14] and can output control force in two directions only by changing the size of electric current.

To ensure the rapidity and effectiveness of the active control strategy for the horizontal vibration of the elevator car, the control method is significant for the active control system. Feng et al.[15,16] established the dynamic spatial model of elevator car horizontal vibration, designed a robust control strategy, and verified the vibration effect by simulation method. Chang et al.[17] studied output feedback control of high-speed elevator systems based on H∞ control. Chen et al.[18,19] proposed a hybrid H_2/H∞ optimal performance preserving state feedback control strategy by establishing state space equations using the LFT method for the phenomenon of horizontal vibration in an elevator car system due to uneven guide rails. Cao et al.[20] designed a robust controller for high-speed elevators based on the linear matrix inequality (LMI) optimization technique. Santo et al.[21] studied the horizontal non-linear response of the three degrees of freedom vertical transport model under the deformation excitation of the guide rail and proposed a state-dependent Ricatti equation (SDRE) to reduce vibration. The above traditional control methods can reduce the horizontal vibration of high-speed elevators, but it is challenging to achieve intelligent automatic optimization. He et al.[22] designed a fuzzy neural network intelligent damping controller based on the Mamdani model for the problem of inconsistent horizontal vibration caused by car and guideway excitation during the actual operation of high-speed elevators. Zhang et al.[23] aiming at the uncertainty of the external excitation of the elevator system, designed the BP-PID controller with a linear prediction model

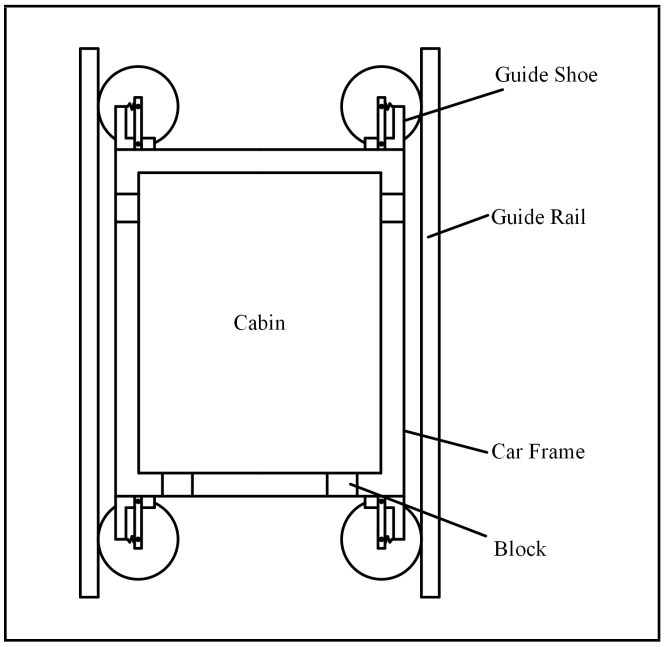

Figure 1. The structure of the elevator car system.

to carry out intelligent active control of the car vibration, and analyzed the effect with MATLAB/Simulink. However, the training process of fuzzy/BP neural networks is tedious, and the learning time is extended, which affects the convergence speed of the adaptive intelligent optimization algorithm. In view of the limitations of the active control method of elevator car horizontal vibration, this paper adopts the linear quadratic controller (LQR) control method to actively control the elevator car horizontal vibration more quickly and effectively. To obtain a better active control effect, an intelligent optimization algorithm based on the particle swarm algorithm (PSO) is proposed to optimize the power coefficient matrix of the LQR optimal controller to attenuate the high-speed elevator horizontal vibration more quickly and timely.

PSO is an optimization algorithm based on birds' predation. When solving complex problems, the original PSO algorithm may not converge to global optimization. Therefore, Shi et al.[24] introduced inertia weight into the original PSO algorithm and proposed the existing basic PSO algorithm. Inertia weight $\mathbf{Q}$ is the most crucial parameter determining the optimization result and convergence speed in the PSO algorithm. Increasing the value of ω can improve the global search ability of the algorithm and make the convergence speed faster; reducing the value of ω can improve the local search ability of the algorithm and make the optimization result better. Therefore, Shu Kai et al.[25] proposed a linear decline of inertia weight particle swarm optimization algorithm, Its inertia weight linear decline of dynamic as the number of iterations increases to improve the optimization effect of the algorithm. Later, scholars also improved the particle swarm optimization algorithm from the optimization result and convergence speed,[26–29] but most can't consider both the convergence speed and optimization effect. In the light of the characteristics of LQR control of elevator car horizontal vibration, to find the weighting coefficient matrix $\mathbf{Q}$ of LQR controller more quickly and effectively, this paper proposes a Jumping inertia Weight Particle Swarm Optimization (JWPSO) algorithm which can adjust the inertia weight of PSO adaptively according to the objective function value and

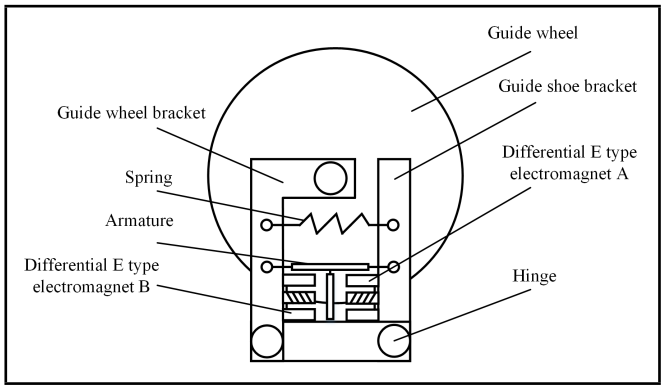

Figure 2. The structure of differential magnetic suspension active guide shoe.

optimizes the weighting matrix $\mathbf{Q}$ of LQR control by using JWPSO to improve further the LQR control effect of elevator car horizontal vibration primary control and then simulates the elevator car horizontal vibration by MATLAB/Simulink to analyze the effect of active control.

The rest of this paper is organized as follows. In Section 2, a differential maglev active guide shoe is designed based on the principle of the maglev system, and the time lag effect of the actuator is described; in Section 3, the dynamics model of the high-speed elevator car system is established; in Section 4, the optimal LQR controller is designed and its stability is verified; in Section 5, the LQR controller is intelligently optimized with the JWPSO algorithm; in Section 6, MatLab software is used to compare the effectiveness of the designed controller in reducing the horizontal vibration of the high-speed elevator car system under different load cases and with other algorithms. Then conclusions are drawn in Section 7.

2. ELEVATOR DIFFERENTIAL MAGNETIC SUSPENSION ACTIVE GUIDE SHOE

2.1. Design of Differential Active Guide Shoe

The elevator car system comprised the cabin, car frame, and guide mechanisms, including guide rail and rolling guide shoe. The structure of the car system is shown in Fig. 1. During the working process of the guide mechanism, the uneven displacement excitation of the guide rail was transmitted to the elevator car through the elevator guide shoe to generate the horizontal vibration of the car. To control the horizontal vibration of the elevator car more quickly and effectively in the elevator car system structure, in this section, designed a differential magnetic suspension active guide shoe based on the principle of differential magnetic suspension actuator.

The structure of the differential magnetic suspension active guide shoe is shown in Fig. 2. The active guide shoe comprised a differential magnetic suspension actuator, guide shoe spring, guide wheel, guide wheel bracket, and guide shoe bracket. When the guide shoe is not working, the armature of the magnetic suspension actuator is in the middle position under the restriction of the guide shoe spring. When the elevator car has vibration displacement under the excitation of the guide rail, the armature of the magnetic suspension actuator is separated from the middle position. Then, the control system determines the corresponding differential electromagnetic force through

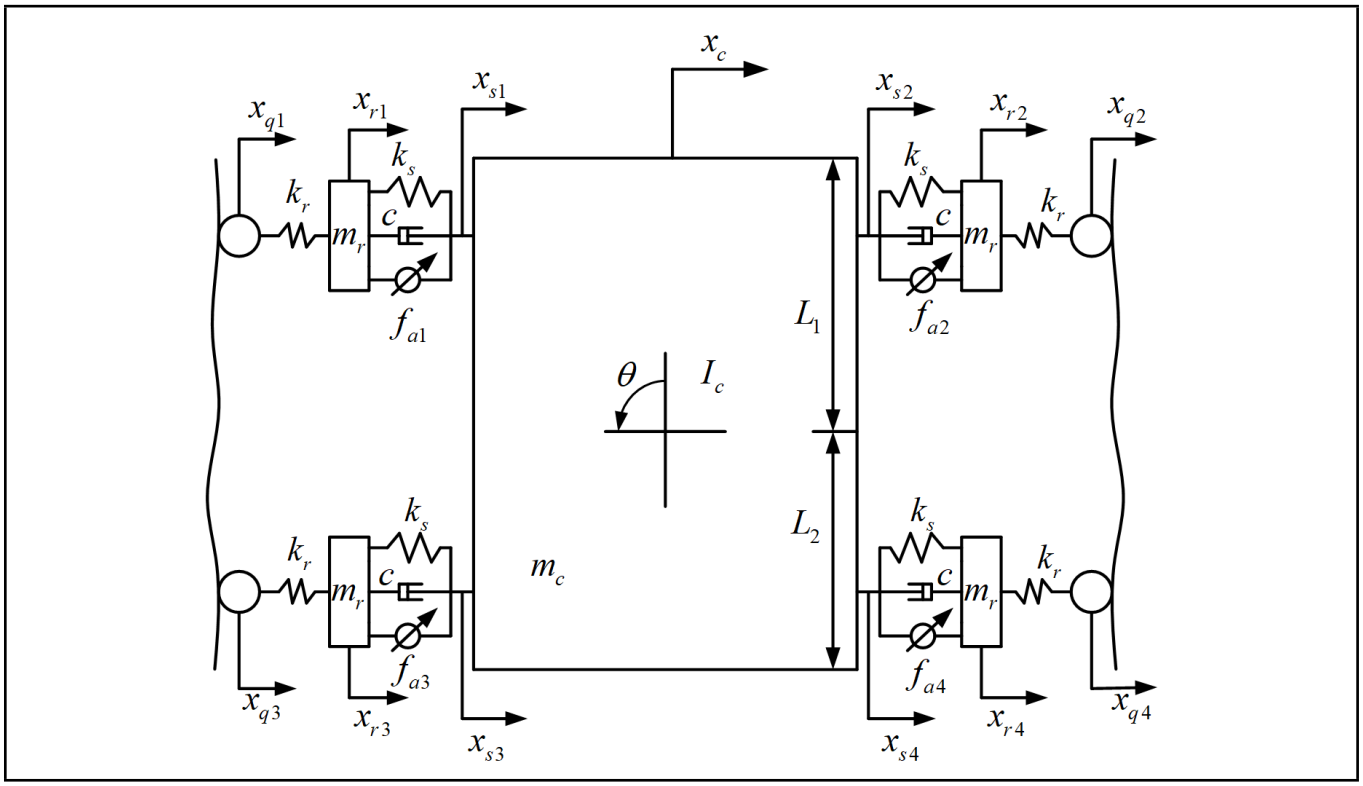

Figure 3. The horizontal vibration dynamic model of high-speed elevator car with differential magnetic suspension active guide shoe under the excitation of the guide rail.

the vibration state to control the horizontal vibration of the elevator car. So, the differential magnetic suspension actuator and guide shoe spring offset the horizontal vibration of the elevator car through active vibration isolation and passive vibration isolation, respectively.

The electromagnetic force f_a produced by the magnetic suspension actuator is related to the current and the air gap distance between the armature iron and the electromagnet.[14] The mathematical relationship was as follows:

$$f_a = k_m \left(\frac{i_1^2}{(x_0 + x)^2} - \frac{i_2^2}{(x_0 - x)^2} \right); \tag{1}$$

where

$$k_m = \frac{\mu_0 N^2 S}{4};$$

where μ_0 was the permeability in the air, N was the number of turns of winding coil, S was the area of electromagnet pole, i_1 and i_2 represented the electric current of the differential E-type electromagnets A and B, respectively, x_0 indicated the air gap distance between the armature and differential electromagnets A and B when the magnetic suspension actuator was in the middle position when it was not working. x was the amount of air gap the same as armature displacement.

2.2. Description of Time Delay Effect of Actuator

In the process of reducing the vibration of the car system, it takes a specific time for the vibration signal picked up by the vibration sensor to be transmitted to the controller, and also takes a certain time for the electric current transferred to the active guide shoe driven by the controller, so there will be a time delay phenomenon when the active guide shoe is activated.

To describe the time delay phenomenon of the actuator more comprehensively and simply, we make the following assumptions:

1. The signal transmission delay of the sensor only comes from the deviation from the transmission time of the electrical signal, and the deviation is τ_1;
2. The time transfer deviation of the electric signal of the actuator is τ_2.

According to the above assumptions, the equivalent delay deviation of the actuator is as:

$$\tau = \tau_1 + \tau_2.$$

The electromagnetic force Eq (1) can be rewritten as:

$$f_a(t-\tau) = k_m \left(\frac{i_1(t-\tau)^2}{(x_0 + x)^2} - \frac{i_2(t-\tau)^2}{(x_0 - x)^2} \right). \tag{2}$$

3. DYNAMIC MODEL OF ACTIVE CONTROL FOR HORIZONTAL VIBRATION OF THE ELEVATOR CAR

In the process of high-speed elevator operation, the primary sources of horizontal vibration were the unevenness of the guide rail and the installation error of the guide rail. The horizontal vibration dynamic model of a high-speed elevator car with a differential magnetic suspension active guide shoe under the excitation of the guide rail is established in Fig. 3.

The mass of the car in Fig. 3 was m_c, the moment of inertia was I_c, the distance from the center of mass to the upper and lower active guide shoes was L_1 and L_2 respectively, k_s was stiffness of guide shoe, c_s represented guide shoe damping,

m_r was the mass of the guide shoe, k_r was the contact rigidity of the guide wheel, f_{ai} $(i = 1, 2, 3, 4)$ was the output control force of magnetic suspension actuator, x_c represented the horizontal displacement of the elevator center of mass, θ indicated the angle of the lift car around the center of mass, x_r was the horizontal displacement of the guide shoe, x_{qi} represented the displacement excitation of the guide rail to guide shoe.

Select the generalized coordinates of the system as $q = (x_c, \theta, x_{r1}, x_{r2}, x_{r3}, x_{r4})$, let the kinetic energy and potential energy of the system be T and V. Then the Lagrange function of the system is:

$$L = T - V. \tag{3}$$

The Lagrange equation of the system was:

$$\frac{d}{dt}\left(\frac{\partial L}{\partial \dot{q}_j}\right) - \frac{\partial L}{\partial q_j} + \frac{\partial \varphi}{\partial \dot{q}_j} = Q_j; \tag{4}$$

where φ represented the Rayleigh dissipation function, Q_j $(j = 1, 2, 3, 4, 5, 6)$ expressed the q_j $(j = 1, 2, 3, 4, 5, 6)$ corresponded generalized force. From the Lagrange equation of the system, the dynamic equation of the system was obtained as follows:

$$\begin{cases} m_c\ddot{x}_c = -4k_s x_c + (2k_sL_1 - 2k_sL_2)\theta - 4c_s\dot{x}_c + \\ \quad (2c_sL_1 - 2c_sL_2)\dot{\theta} + k_s(x_{r1} + x_{r2} + x_{r3} + x_{r4}) + \\ \quad c_s(\dot{x}_{r1} + \dot{x}_{r2} + \dot{x}_{r3} + \dot{x}_{r4}) + f_{a1} + f_{a2} + f_{a3} + f_{a4}; \\ I_c\ddot{\theta} = (2L_1 - 2L_2)k_s x_c - (2L_1^2 + 2L_2^2)k_s\theta + \\ \quad (2L_1 - 2L_2)c_s\dot{x}_c - (2L_1^2 + 2L_2^2)c_s\theta - L_1k_sx_{r1} - \\ \quad L_1k_sx_{r2} + L_2k_sx_{r3} + L_2k_sx_{r4} - L_1c_s\dot{x}_{r1} - \\ \quad L_1c_s\dot{x}_{r2} + L_2c_s\dot{x}_{r3} + L_2c_s\dot{x}_{r4} - L_1f_{a1} - L_1f_{a2} + \\ \quad L_2f_{a3} + L_2f_{a4}; \\ m_r\ddot{x}_{r1} = k_sx_c - k_sL_1\theta + c_s\dot{x}_c - c_sL_1\dot{\theta} - \\ \quad (k_s + k_r)x_{r1} - c_s\dot{x}_{r1} + k_rx_{q1} - f_{a1}; \\ m_r\ddot{x}_{r2} = k_sx_c - k_sL_1\theta + c_s\dot{x}_c - c_sL_1\dot{\theta} - \\ \quad (k_s + k_r)x_{r2} - c_s\dot{x}_{r2} + k_rx_{q2} - f_{a2}; \\ m_r\ddot{x}_{r3} = k_sx_c + k_sL_2\theta + c_s\dot{x}_c + c_sL_2\dot{\theta} - \\ \quad (k_s + k_r)x_{r3} - c_s\dot{x}_{r3} + k_rx_{q3} - f_{a3}; \\ m_r\ddot{x}_{r4} = k_sx_c + k_sL_2\theta + c_s\dot{x}_c + c_sL_2\dot{\theta} - \\ \quad (k_s + k_r)x_{r4} - c_s\dot{x}_{r4} + k_rx_{q4} - f_{a4}. \end{cases} \tag{5}$$

Select state variable was:
$\mathbf{X} = (x_c, \theta, \dot{x}_c, \dot{\theta}, x_{r1}, x_{r2}, x_{r3}, x_{r4}, \dot{x}_{r1}, \dot{x}_{r2}, \dot{x}_{r3}, \dot{x}_{r4})^T$, the output variable was: $\mathbf{Y} = (x_c, \theta, x_{r1}, x_{r2}, x_{r3}, x_{r4}, \ddot{x}_c, \ddot{\theta})^T$, the control variable was: $\mathbf{U} = (f_{a1}, f_{a2}, f_{a3}, f_{a4})^T$, the guide excitation was: $\mathbf{W} = (x_{q1}, x_{q2}, x_{q3}, x_{q4}, \dot{x}_{q1}, \dot{x}_{q2}, \dot{x}_{q3}, \dot{x}_{q4})^T$. The dynamic equation was transformed into the state-space expression:

$$\begin{cases} \dot{\mathbf{X}} = \mathbf{A}\mathbf{X} + \mathbf{B}\mathbf{U} + \mathbf{R}\mathbf{W}; \\ \mathbf{Y} = \mathbf{C}\mathbf{X} + \mathbf{D}\mathbf{U}; \end{cases} \tag{6}$$

where the matrices $\mathbf{A}$ to $\mathbf{D}$ are given in the Appendix.

In the process of passengers being transported to each floor, the vibration caused by the guide rail excitation was transmitted to the human body through the bottom of the car, thus affecting the comfort of passengers taking the elevator. Therefore, the horizontal vibration acceleration at the center of the car bottom was regarded as the observation index. If the horizontal vibration acceleration at the center of the car bottom was a, the expression was:

$$a = \ddot{x}_c + L_2\ddot{\theta}. \tag{7}$$

4. THE DESIGN OF THE LQR CONTROLLER FOR THE HORIZONTAL VIBRATION OF THE CAR

4.1. The Design of the LQR Controller

LQR control was a mature and widely used control method in modern control theory. The control system's output variable or state variable was weighted to set the control system's value function. The system's optimal feedback gain matrix was obtained by solving the Ricatti matrix algebraic equation to realize the optimal control of the system. In the high-speed elevator car horizontal vibration active control system, the output variable was: $\mathbf{Y} = (x_c, \theta, x_{r1}, x_{r2}, x_{r3}, x_{r4}, \ddot{x}_c, \ddot{\theta})^T$, therefore, the value function of the control system was:

$$J_1 = \int_0^\infty \Big(q_1x_c^2 + q_2\theta^2 + q_3x_{r1}^2 + q_4x_{r2}^2 + q_5x_{r3}^2 + q_6x_{r4}^2 + q_7\ddot{x}_c^2 + q_8\ddot{\theta}^2\Big)\,dt. \tag{8}$$

Translate into matrix formula was as follows:

$$J_1 = \int_0^\infty \left(\mathbf{Y}^T\mathbf{Q}_1\mathbf{Y}\right)dt; \tag{9}$$

where $\mathbf{Q}_1 = \mathrm{diag}(q_1, q_2, q_3, q_4, q_5, q_6, q_7, q_8)$ was a half positive definite matrix, q_i $(i = 1, \ldots, 8)$ was the output weighting coefficient of elevator car horizontal vibration active control. Since the output active control force of the differential magnetic suspension actuator had a specific range, to meet the active control ability of the output control force of the actuator to the vibration system, the active control force should be weighted limited, so the value function of the system should also be modified to:

$$J = \int_0^\infty \left(\mathbf{Y}^T\mathbf{Q}_1\mathbf{Y} + \mathbf{U}^T\mathbf{R}_1\mathbf{U}\right)dt; \tag{10}$$

where $\mathbf{R}_1 = \mathrm{diag}(r_1, r_2, r_3, r_4)$ was a positive definite matrix, r_i $(i = 1, 2, 3, 4)$ was the weighting coefficient of the output control force of the differential magnetic suspension actuator.

According to the state-space Eq. (6), the value function can be rewritten as:

$$\begin{aligned} J &= \int_0^\infty \left(\mathbf{Y}^T\mathbf{Q}_1\mathbf{Y} + \mathbf{U}^T\mathbf{R}_1\mathbf{U}\right)dt \\ &= \int_0^\infty \left((\mathbf{C}\mathbf{X}+\mathbf{D}\mathbf{U})^T\mathbf{Q}_1(\mathbf{C}\mathbf{X}+\mathbf{D}\mathbf{U}) + \mathbf{U}^T\mathbf{R}_1\mathbf{U}\right)dt \\ &= \int_0^\infty \Big(\mathbf{X}^T\mathbf{C}^T\mathbf{Q}_1\mathbf{C}\mathbf{X} + \mathbf{X}^T\mathbf{C}^T\mathbf{Q}_1\mathbf{D}\mathbf{U} + \\ &\qquad \mathbf{U}^T\left(\mathbf{R}_1+\mathbf{D}^T\mathbf{Q}_1\mathbf{D}\right)\mathbf{U}\Big)\,dt. \end{aligned} \tag{11}$$

That is:

$$J = \int_0^\infty \left(\mathbf{X}^T\mathbf{Q}\mathbf{X} + 2\mathbf{X}^T\mathbf{N}\mathbf{U} + \mathbf{U}^T\mathbf{R}\mathbf{U}\right)dt; \tag{12}$$

where $\mathbf{Q} = \mathbf{C}^T\mathbf{Q}_1\mathbf{C}$, $\mathbf{N} = \mathbf{C}^T\mathbf{Q}_1\mathbf{D}$, $\mathbf{R} = \mathbf{R}_1 + \mathbf{D}^T\mathbf{Q}_1\mathbf{D}$.

According to the principle of extremum, when the system value function takes the minimum value, the ideal optimal control can be obtained as follows:

$$\mathbf{U} = -\mathbf{R}^{(-1)}\left(\mathbf{N}^T + \mathbf{B}^T\mathbf{P}\right)\mathbf{X} = -\mathbf{K}\mathbf{X}; \tag{13}$$

where $\mathbf{K}$ was the optimal feedback matrix, $\mathbf{P}$ was the only positive definite solution of Ricatti algebraic equation:

$$\mathbf{P}\mathbf{A} + \mathbf{A}^T\mathbf{P} - \mathbf{N}\mathbf{R}^{(-1)}\mathbf{B}^T\mathbf{P} - \mathbf{P}\mathbf{B}\mathbf{R}^{(-1)}\mathbf{N}^T - \mathbf{P}\mathbf{B}\mathbf{R}^{(-1)}\mathbf{B}^T\mathbf{P} - \mathbf{N}\mathbf{R}^{(-1)}\mathbf{N}^T + \mathbf{Q} = \mathbf{0}. \tag{14}$$

4.2. Stability Conditions of LQR Controller

Theorem: For system Eq. (6), the LQR controller was asymptotically stable under the following conditions:

$$\mathbf{Q} - \mathbf{N}\mathbf{R}^{(-1)}\mathbf{N}^T \geq \mathbf{0}. \tag{15}$$

Proof: Suppose Lyapunov function as:

$$\mathbf{V}(\mathbf{X}) = \mathbf{X}^T\mathbf{P}\mathbf{X}. \tag{16}$$

Then $\mathbf{V}(\mathbf{X})$ was a positive definite function, and its first derivative was:

$$\begin{aligned}\dot{\mathbf{V}}(\mathbf{X}) &= \dot{\mathbf{X}}^T\mathbf{P}\mathbf{X} + \mathbf{X}^T\mathbf{P}\dot{\mathbf{X}} \\ &= \mathbf{X}^T\Big(\mathbf{P}\mathbf{A} + \mathbf{A}^T\mathbf{P} - \mathbf{N}\mathbf{R}^{(-1)}\mathbf{B}^T\mathbf{P} - \\ &\quad \mathbf{P}\mathbf{B}\mathbf{R}^{(-1)}\mathbf{N}^T - 2\mathbf{P}\mathbf{B}\mathbf{R}^{(-1)}\mathbf{B}^T\mathbf{P}\Big)\mathbf{X}.\end{aligned} \tag{17}$$

Introduce the Ricatti algebraic Eq. (15) into Eq. (17), which was as follows:

$$\dot{\mathbf{V}}(\mathbf{X}) = -\mathbf{X}^T\big(\mathbf{Q} + \mathbf{P}\mathbf{B}\mathbf{R}^{(-1)}\mathbf{B}^T\mathbf{P} - \mathbf{N}\mathbf{R}^{(-1)}\mathbf{N}^T\big)\mathbf{X}. \tag{18}$$

To make the system gradually stable:

$$\begin{aligned}&\dot{\mathbf{V}}(\mathbf{X}) \prec \mathbf{0}; \\ &\mathbf{Q} - \mathbf{N}\mathbf{R}^{(-1)}\mathbf{N}^T \geq \mathbf{0}.\end{aligned} \tag{19}$$

4.3. Output Delay Compensation of Electromagnetic Control Force

Suppose that the control force f_{ai} $(i = 1, 2, 3, 4)$ solved by LQR in Section 4.1 is transmitted to the active guide shoe, and the actual time-delay active control force f'_{ai} obtained is:

$$f'_{ai} = \begin{cases} f_{ai}(t-\tau), & \text{when } x_{si} - x_{ri} \neq 0; \\ 0, & \text{else.} \end{cases} \tag{20}$$

To enhance the vibration suppression effect of the designed control force, at the time t, predict active control force at time $t+\tau$ is as $f_{ai}(t+\tau) = f_{pi}$. When τ is very small, the first-order Taylor expansion equation of f_{pi} at $\tau = 0$ is as follows:

$$f'_{ai} = \begin{cases} f_{ai}(t+\tau) = f_{ai}(t) + \tau\dot{f}_{ai}(t), & \text{when } x_{si} - x_{ri} \neq 0; \\ 0, & \text{else;} \end{cases} \tag{21}$$

where f_{pi} is the compensation control force at time t, the control vector is: $\mathbf{U}_p = [f_{p1}, f_{p2}, f_{p3}, f_{p4}]^T$. Then Eq. (4) can be rewritten as follows:

$$\begin{cases} \dot{\mathbf{X}} = \mathbf{A}\mathbf{X}(t) + \mathbf{B}\mathbf{U}_p(t) + \mathbf{R}\mathbf{W}; \\ \mathbf{Y} = \mathbf{C}\mathbf{X}(t) + \mathbf{D}\mathbf{U}_p(t). \end{cases} \tag{22}$$

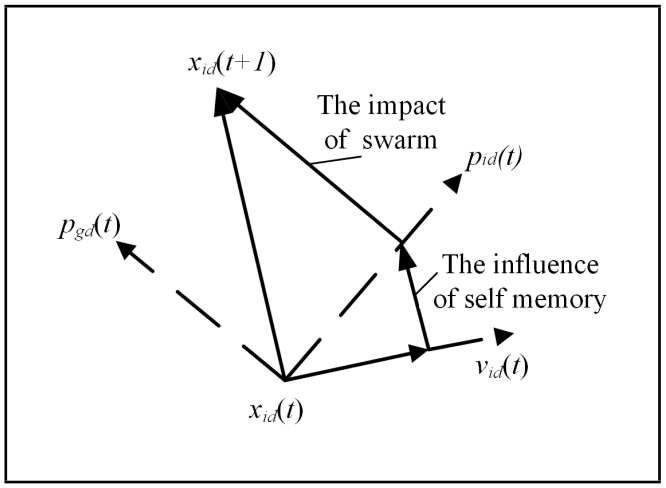

Figure 4. Update mode of the optimal particle position.

From Eqs. (13) and (21), it can be concluded that:

$$\mathbf{U}_p = \mathbf{K}\mathbf{X} + \tau\mathbf{K}\dot{\mathbf{X}}. \tag{23}$$

When designing controller, ignoring external excitation:

$$\dot{\mathbf{X}} = \mathbf{A}\mathbf{X} - \mathbf{B}\mathbf{K}\mathbf{X}. \tag{24}$$

The expression of compensation control variable can be rewritten as:

$$\begin{aligned}\mathbf{U}_p &= -\mathbf{K}\mathbf{X} - \tau\mathbf{K}(\mathbf{A}\mathbf{X} - \mathbf{B}\mathbf{K}\mathbf{X}) \\ &= -(\mathbf{K} + \tau\mathbf{K}\mathbf{A} - \tau\mathbf{K}\mathbf{B}\mathbf{K})\mathbf{X}.\end{aligned} \tag{25}$$

5. THE OPTIMIZATION IMPROVEMENT OF LQR CONTROL BY JWPSO

5.1. Jumping Inertia Weight Particle Swarm Optimization

Particle swarm optimization (PSO) is an optimization algorithm that guides the optimization search through the swarm intelligence generated by the cooperation and competition among the particles in the swarm.

In the PSO algorithm, the potential solution of every optimization problem is a particle in space. All particles have a fitness value determined by the fitness function. Each particle has a speed to determine its flight direction and distance. The algorithm is initialized as a group of random solutions, and then the optimal solution is found through iteration. In a D-dimensional search space, there is a community composed of N particles, where the position of the i-th $(i = 1, 2, 3, \ldots, N)$ particle is a D-dimensional vector: $\mathbf{X}_i = (x_{i1}, x_{i2}, x_{i3}, \ldots, x_{iD})$, its speed is: $\mathbf{V}_i = (v_{i1}, v_{i2}, v_{i3}, \ldots, v_{iD})$, the individual optimal position searched by the particle is: $\mathbf{P}_{\text{best}} = (p_{i1}, p_{i2}, p_{i3}, \ldots, p_{iD})$, the particle swarm searched the global optimal position is: $\mathbf{G}_{\text{best}} = (p_{g1}, p_{g2}, p_{g3}, \ldots, p_{gD})$, The update mode of the optimal particle position is shown in Fig. 4.

After finding the current individual optimal value and global optimal value, particles update their speed and position accord-

Table 1. Data of Griewank function optimization effect under PSO algorithm and JWPSO algorithm.

Iterative step	50	100	150	200	250	300
PSO	0.2548	0.1426	0.0381	0.0406	0.1035	0.0259
JWPSO	4.2596e-8	7.1039e-11	2.82e-14	0	0	0

Table 2. Data of Rastrigin function optimization effect under PSO algorithm and JWPSO algorithm.

Iterative step	50	100	150	200	250	300
PSO	14.0261	7.7225	10.9805	16.0609	26.3548	2.7199
JWPSO	1.7859	0.9963	2.9849	1.229e-9	8.136e-13	2.948e-13

ing to the following formula:

$$\begin{cases} v_{id}(t+1) = \omega^* v_{id}(t) + c_1 r_1 \big(p_{id}(t) - x_{id}(t)\big) + \\ \qquad\qquad c_2 r_2 \big(p_{id}(t) - x_{id}(t)\big); \\ x_{id}(t+1) = x_{id}(t) + vid(t+1); \end{cases} \tag{26}$$

where ω was the inertia weight, the value range usually was $[0.2, 1.2]$, c_1 and c_2 was a learning factor, its value range is $[0, 4]$, r_1 and r_2 is the random uniform number in the range $[0, 1]$.

In the PSO algorithm, for some particles with high fitness, such as p, there may be a point p_x in the local region to update the global optimum. That is to say, the solution represented by p_x was better than the current global optimal solution. Therefore, in the region near p, the inertia weight ω should be reduced to enhance its local search ability to quickly update the global optimal p_x. For the particles with poor adaptability, the inertia weight ω should be appropriately increased to skip the current region swiftly to enhance the global search ability and accelerate the convergence speed.

To make PSO search the output optimal weighting matrix $\mathbf{Q}$ of LQR control quickly and accurately, this section proposed a Jumping inertia Weight Particle Swarm Optimization (JWPSO) algorithm to optimize the output weighting coefficient matrix $\mathbf{Q}$ of LQR control. The improved method of inertia weight is weight adaptive jump update. The weight update formula is:

$$\omega = \begin{cases} \omega_{\max} - \frac{(\omega_{\max} - \omega_{\min})v}{2M} * \frac{(f_{\text{avg}} - f_{\min})}{(f_{\max} - f_{\min})}, & f_{\text{avg}} \le f; \\ \omega_{\min}, & f_{\text{avg}} > f; \end{cases} \tag{27}$$

where $\omega_{\max}$ was the maximum value of the current inertia weight, and $\omega_{\min}$ was the minimum value of the current inertia weight, f_{avg} was the average value of the fitness function of the current particle population, and $f_{\max}$, $f_{\min}$ were the maximum and minimum values of the fitness function of the current particle population separately. M are the maximum iteration steps, and v are the current iteration steps.

From the inertia weight jumping update Eq. (21), it can be seen the optimization principle of the JWPSO algorithm:

1. When the current fitness function value f of particles was more significant (more remarkable than the average value), the inertia weight of particles decreases slightly with the increase of iteration steps so that the algorithm can quickly skim the solution with smaller fitness and accelerate the convergence speed;

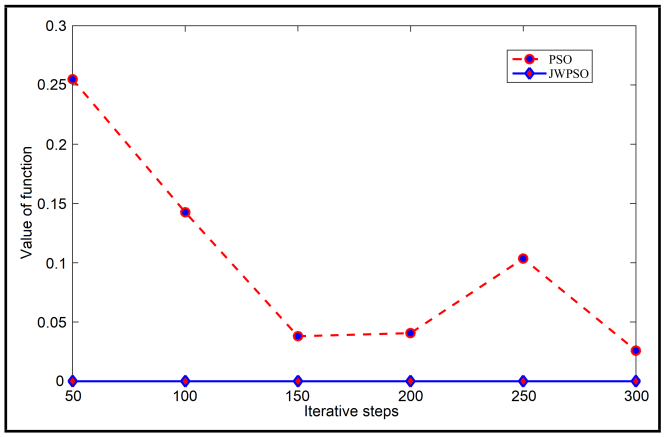

Figure 5. The comparison diagram of Griewank function optimization effect under PSO algorithm and JWPSO algorithm.

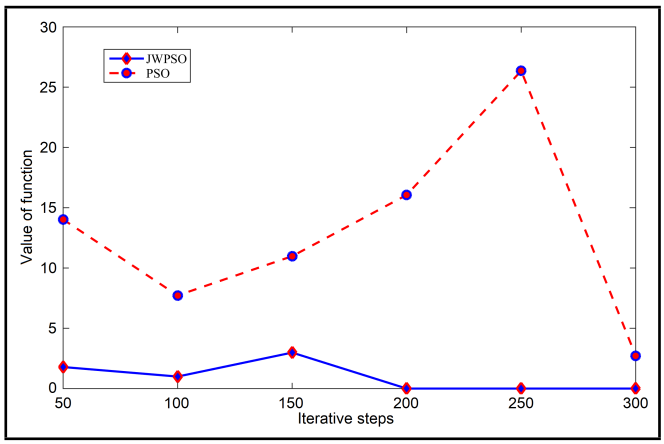

Figure 6. The comparison diagram of Rastrigin function optimization effect under PSO algorithm and JWPSO algorithm.

2. When the current fitness function value f of the particle is small (less than the average value), the inertia weight is directly updated to the minimum value for local search to ensure the optimization results of the particle swarm optimization algorithm.

To verify the validity of the JWPSO algorithm, use the PSO algorithm and JWPSO algorithm respectively to search for the minimum values of the Griewank function and Rastrigin function when the iteration steps of the algorithm are 50, 100, 150, 200, 250, and 300. The optimization results are shown in Table 1 and Table 2. The comparison diagram of the optimization results are made from the optimization results data are shown in Fig. 5 and Fig. 6.

The results in the figures and tables mentioned above show that the JWPSO algorithm can find the minimum value of the test function more accurately than the PSO algorithm; the optimization results of the JWPSO algorithm are better than the PSO algorithm.

5.2. Optimization of Active Control of Horizontal Vibration of Elevator Car by JWPSO

In the active control of horizontal vibration of the high-speed elevator car, the weighting coefficient matrix $\mathbf{Q}$ is related to the output weighting matrix $\mathbf{Q}_1$; therefore, the value of output weighting matrix $\mathbf{Q}_1$ is the key to designing LQR controller,

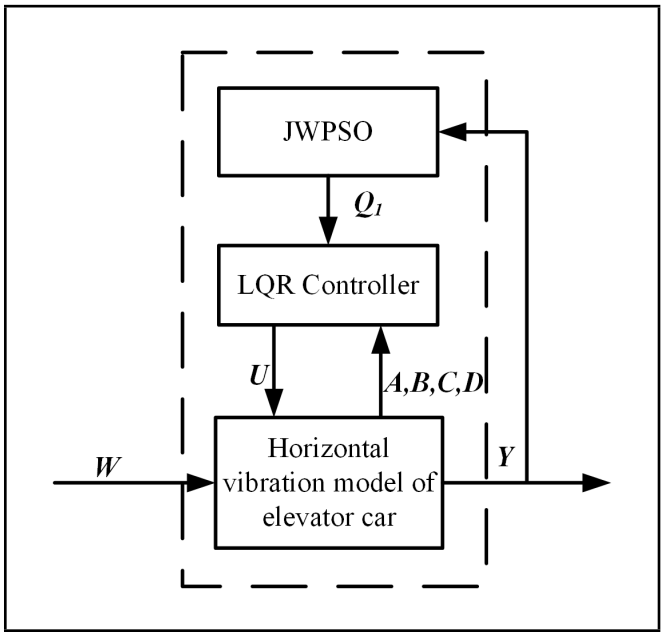

Figure 7. The elevator car horizontal vibration active control strategy.

using the JWPSO algorithm to optimize the LQR control output weighting coefficient matrix $\mathbf{Q}_1$ intelligently. The elevator car horizontal vibration active control strategy is shown in Fig. 7.

The purpose of optimizing the output weighting matrix $\mathbf{Q}_1$ of LQR control is to reduce the horizontal vibration displacement x and acceleration $\ddot{x}$ car mass center of the high-speed, as well as the rotation angle θ and rotation acceleration $\ddot{\theta}$ of the car around the center of mass. Therefore, the fitness function of the JWPSO algorithm is selected as:

$$f_{adp} = \frac{x_{c\_cor}(\mathbf{Q}_1)}{x_{c\_nor}} + \frac{\theta_{c\_cor}(\mathbf{Q}_1)}{\theta_{c\_nor}} + \frac{\ddot{x}_{c\_cor}(\mathbf{Q}_1)}{\ddot{x}_{c\_nor}} + \frac{\ddot{\theta}_{c\_cor}(\mathbf{Q}_1)}{\ddot{\theta}_{c\_nor}}; \tag{28}$$

where x_{c_cor} and θ_{c_cor} represented the root mean square (RMS) of vibration displacement in the horizontal direction of car barycenter and the RMS of car rotation around barycenter after active control, and $\ddot{x}_{c\_cor}$, $\ddot{\theta}_{c\_cor}$ represented the RMS of the horizontal vibration acceleration of the car center of mass and the RMS of the rotation angular acceleration of the car around the center of mass after the active control. x_{c_nor} and θ_{c_nor} represented the RMS of vibration displacement in the horizontal direction of car barycenter and the RMS of car rotation around barycenter without active control, and $\ddot{x}_{c\_nor}$, $\ddot{\theta}_{c\_nor}$ represented the RMS of the horizontal vibration acceleration of the car center of mass and the RMS of the rotation angular acceleration of the car around the center of mass without active control. According to formula Eq. (22), when the fitness function f_{adp} of the JWPSO algorithm gets the minimum value, the output weighting coefficient matrix $\mathbf{Q}_1$ can achieve the best control effect of LQR. Therefore, it can better restrain the horizontal vibration of the elevator car.

Table 3. Simulation parameters of elevator car horizontal vibration active control.

Parameter	Unit	Value	Parameter	Unit	Value
m_c	kg	2.5e3	k_r	N/m	6e5
I_c	kgm^2	3e3	L_1	m	1.7
k_s	N/m	5e5	L_2	m	1.3
c_s	Ns/m	920	m_r	kg	25

6. SIMULATION OF JWPSO-TDLQR TO CONTROL THE ELEVATOR CAR HORIZONTAL VIBRATION

The 4 m/s high-speed elevator was taken as the simulation experiment object in this section. Gaussian white noise is used as the elevator guide excitation,[30] and the simulation experiments are conducted under the excitation. The simulation experiment parameters of the 4 m/s high-speed elevator car horizontal vibration system are shown in Table 3.

To verify the tracking effect of the proposed time-delay LQR controller based on weight hopping particle swarm optimization (JWPSO-TDLQR), the proposed JWPSO-TDLQR controller and the LQR controller based on weight jumping particle swarm optimization (JWPSO-LQR) in the case of ideal state control was used to control the horizontal vibration of the car system. Furthermore, taking the LQR controller optimized by genetic algorithm and the robust controller based on linear matrix inequality (LMI-H$^\infty$) as the contrast object, the proposed controller's control effect is compared with the control method in the previous research to verify the superiority of the proposed control method.

When JWPSO is used to optimize the LQR controller, the number of particle population was selected as 50, the iteration step was chosen as 100, the minimum inertia weight was $\omega_{\min} = 0.2$, and the maximum inertia weight is $\omega_{\max} = 0.6$. The learning factors were $c_1 = c_2 = 2.1$. The optimization result of the algorithm converged in the fitness function $f_{adp} = 1.67$. At this time, the output LQR output weighting coefficient matrix was:

$$\mathbf{Q}_1 = \mathrm{diag}(0.41\ 0.17\ 0.57\ 0.55\ 0.097\ 1.12\ 1.16\ 1.30) \times 10^8. \tag{29}$$

Select $\mathbf{R}_1 = \mathrm{diag}(4, 4, 4, 4)$, let $\mathbf{Q}_2 = \mathbf{Q} - \mathbf{N}\mathbf{R}^{(-1)}\mathbf{N}^T$, then the eigenvalue vector of $\mathbf{Q}_2$ is:

$$\begin{aligned} \mathbf{eig}(\mathbf{Q}_2) &= (7.9e{+}10,\ 3.7e{+}10,\ 1.1e{+}8,\ 5.3e{+}7,\ 5.6e{+}7, \\ &\quad 1.2e{+}7,\ 1.5e{+}4,\ 7.3e{+}3,\ 0,\ 0,\ 0,\ 0)^T \\ \mathbf{eig}(\mathbf{Q}_2) &\geq \mathbf{0}. \end{aligned} \tag{30}$$

From Eq. (19) $\dot{\mathbf{V}}(\mathbf{X}) < \mathbf{0}$ proved the controller is stable.

6.1. Control Effect of JWPSO-TDLQR and Ideal JWPSO-LQR on Car Horizontal Vibration Under Different Working Conditions

To prove the tracking effect of the JWPSO-TDLQR controller designed in this paper on the control results of the car horizontal vibration under the ideal action, based on the above optimization results, this section compares the control results of the vibration acceleration and displacement by using the designed controller and the JWPSO-LQR controller under the

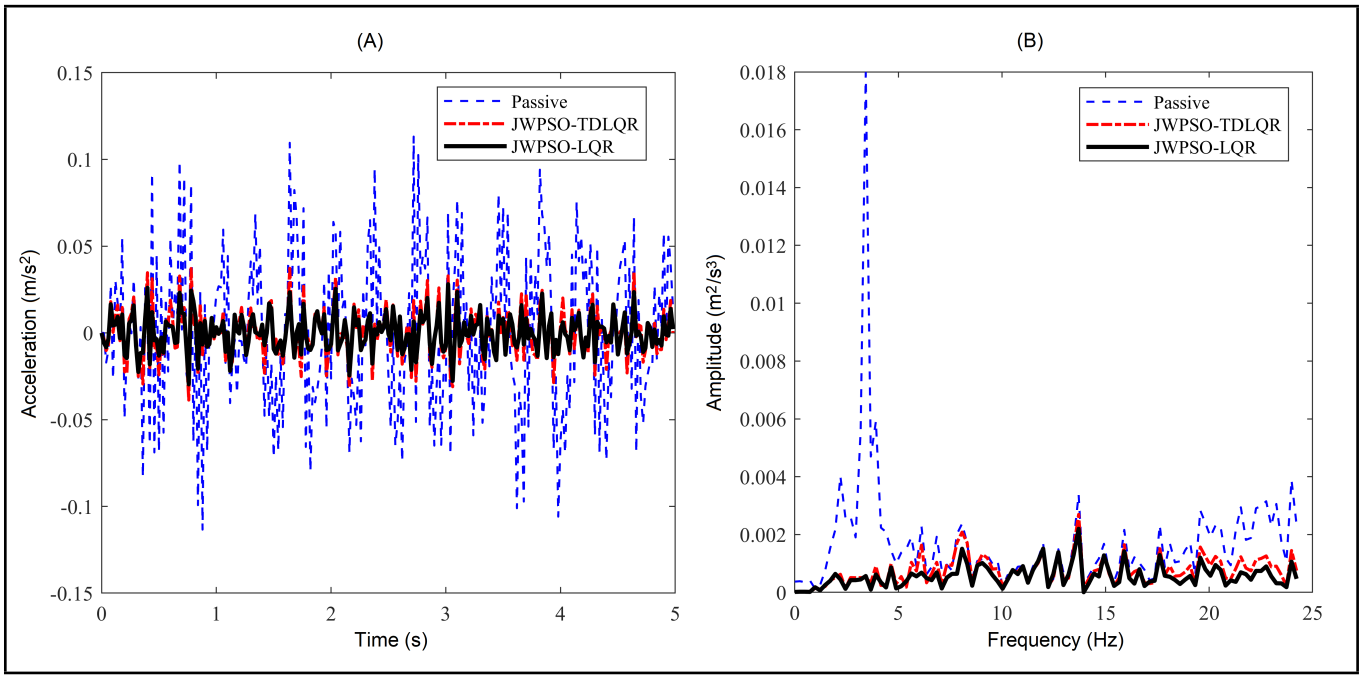

Figure 8. Acceleration response of horizontal vibration of car system with time delay of 2 ms. (A) Time-domain response; (B) Frequency response.

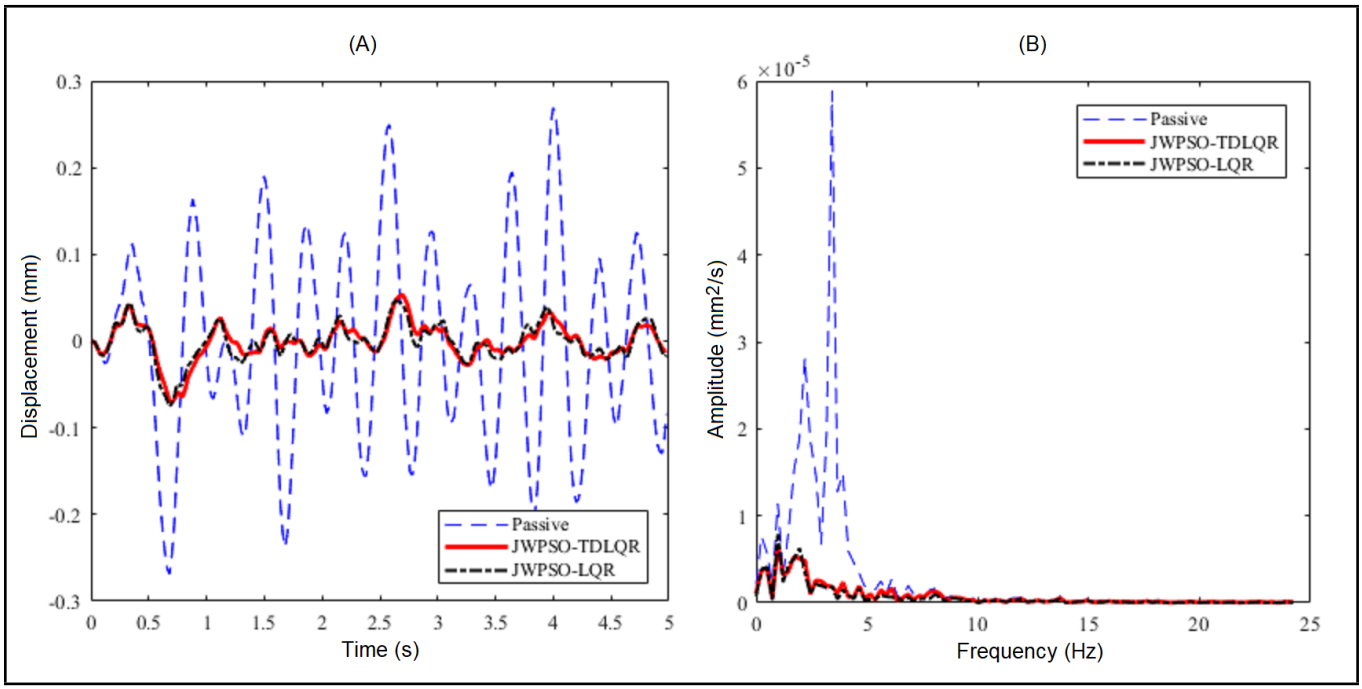

Figure 9. Displacement response of horizontal vibration of car system with time delay of 2 ms. (A) Time-domain response; (B) Frequency response.

ideal state. At the same time, to verify the effectiveness of the designed controller for the mass change during the operation of the elevator, this subsection will ascertain the effectiveness of the designed controller under light load and heavy load conditions, respectively.

The designed controller is applied to track the ideal vibration response when the time delay is 2 ms and 5 ms, respectively. The acceleration and displacement responses of the horizontal vibration under light load cases are shown in Figs. 8–11 for the above two driving delay conditions, respectively.

It can be seen from the vibration response curve that the control effect of JWPSO-TDLQR represented by the red curve is very close to that of the ideal JWPSO-LQR described by the black line no matter in 5 ms or 2 ms time delay. To further show the tracking performance of the proposed controller, the typical numerical characteristics such as maximum value (MAX), root means square (RMS), and peak value in the frequency domain (FP) are shown in Table 4.

According to Table 4, compared with the situation without control, the vibration response under the JWPSO-LQR, the MAX of horizontal vibration acceleration at the bottom center of the elevator car is reduced by 68%, the RMS is reduced by 75%, the FP is reduced by 83%. In the case of 2 ms time delay, under the JWPSO-TDLQR, the MAX is reduced by 62%, the RMS of vibration acceleration is reduced by 73%, the FP is reduced by 80%. In the case of 5 ms time delay, the MAX

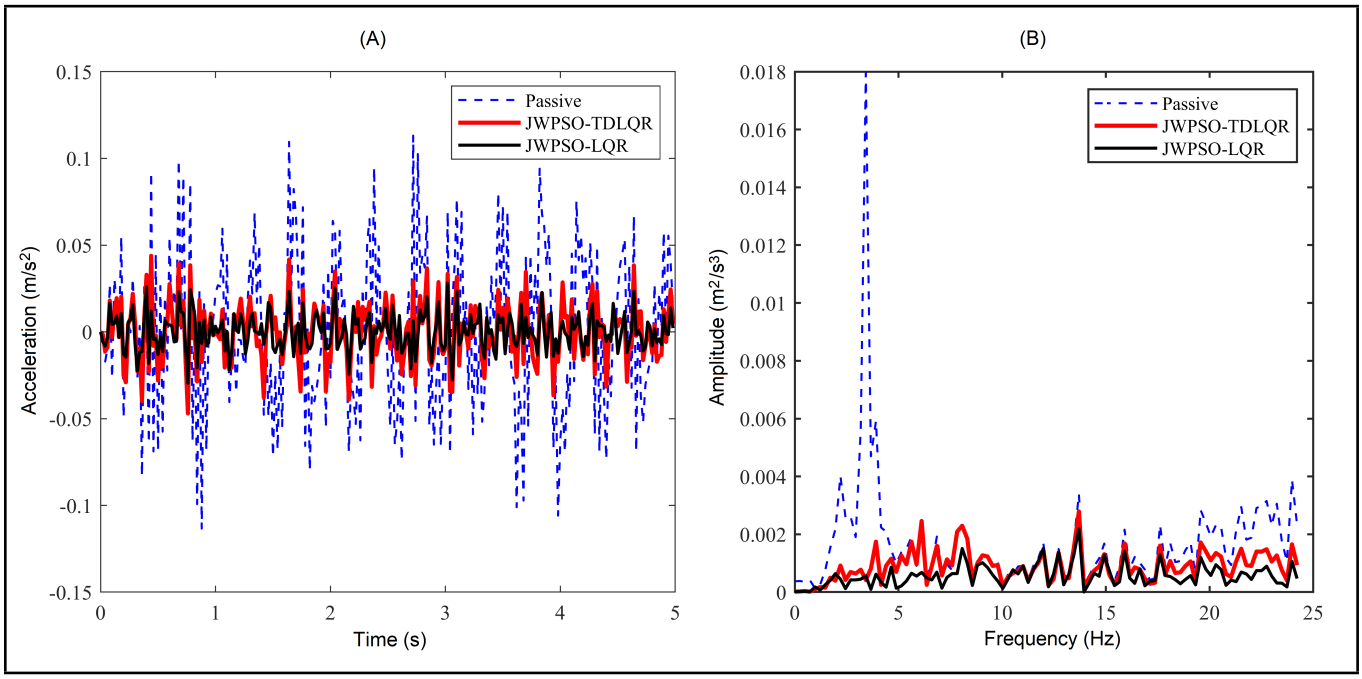

Figure 10. Acceleration response of horizontal vibration of car system with time delay of 5 ms. (A) Time-domain response; (B) Frequency response.

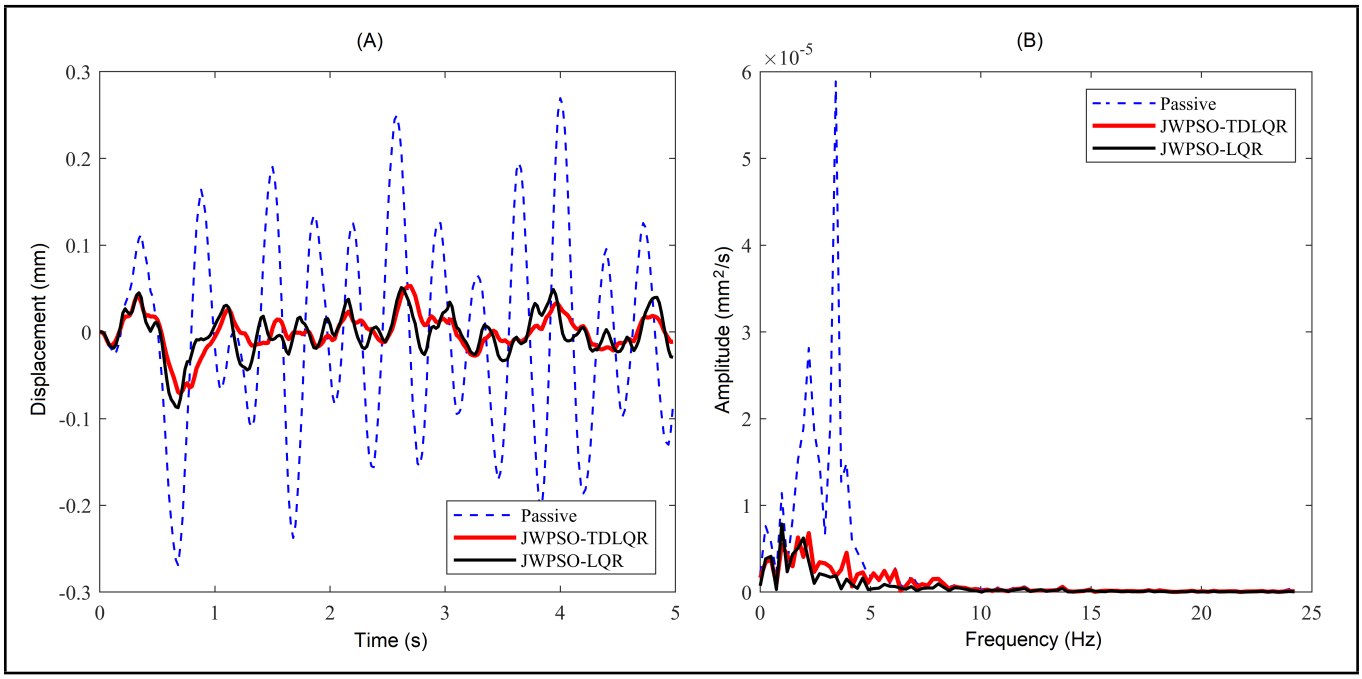

Figure 11. Displacement response of horizontal vibration of car system with time delay of 5 ms. (A) Time-domain response; (B) Frequency response.

is reduced by 60%, the RMS is reduced by 72%, the FP is reduced by 80%. The proposed controller can effectively track the ideal JWPSO-LQR for vibration response reduction under two kinds of time delays, and the difference of typical response characteristics is less than 5%, which proves the effectiveness and robustness of the JWPSO-LQR controller designed in this paper.

Similarly, the designed controller is applied to the ideal vibration response for tracking time delays of 2 ms and 5 ms, respectively, in the heavy load case. The acceleration response and displacement response of the horizontal vibration under different driving conditions are shown in Figs. 12–15, respectively. To further illustrate the tracking performance of the proposed controller, the typical numerical characteristics such as maximum value (MAX), root means square (RMS), and peak value in the frequency domain (FP) are shown in Table 5.

According to Table 5, compared with the situation without control, the vibration response under the JWPSO-LQR, the MAX of horizontal vibration acceleration at the bottom center of the elevator car is reduced by 70%, the RMS is reduced by 76%, the FP is reduced by 86%. In the case of 2 ms time delay, under the JWPSO-TDLQR, the MAX is reduced by 63%, the RMS of vibration acceleration is reduced by 70%, the FP is reduced by 86%. In the case of 5 ms time delay, the MAX is reduced by 63%, the RMS is reduced by 66%, the FP is reduced by 86%. The proposed controller can effectively track

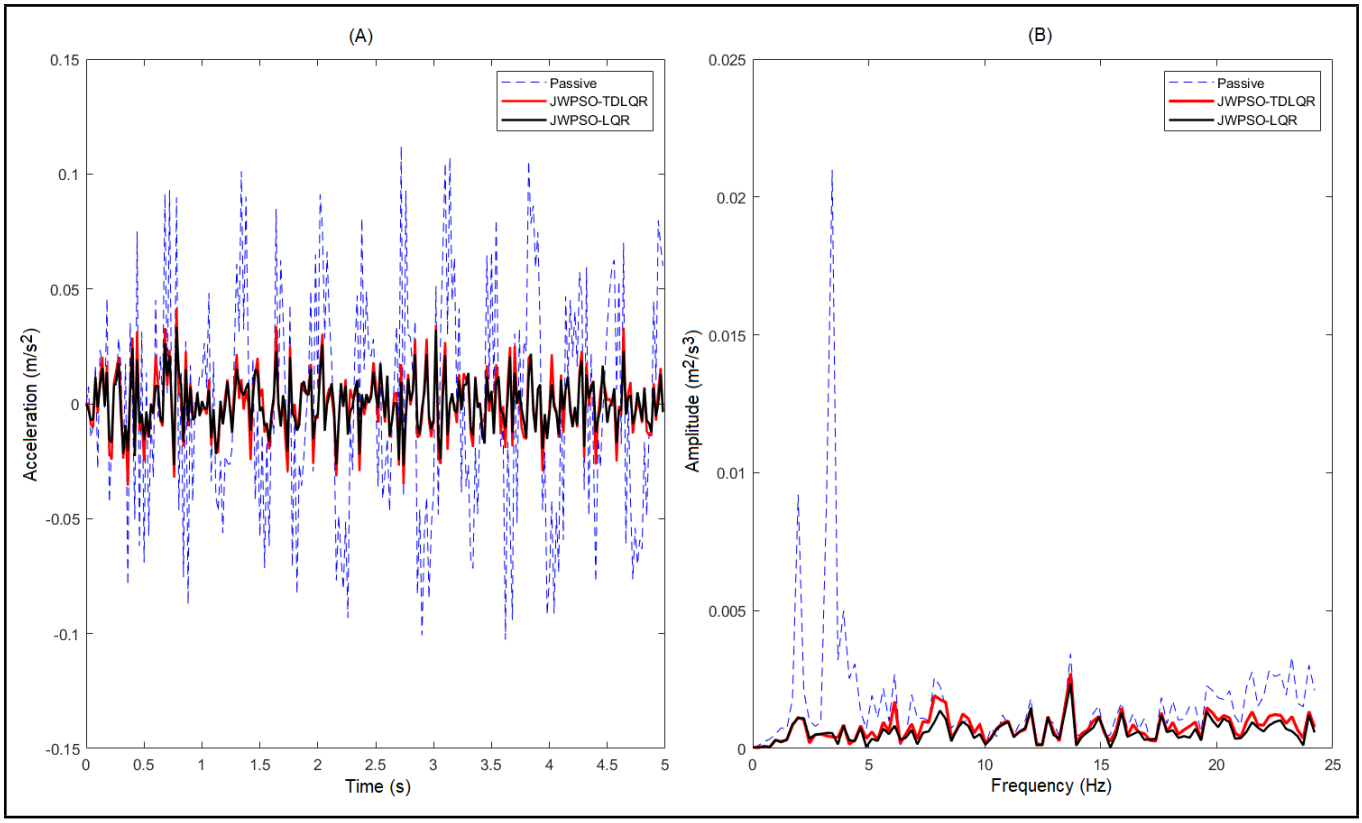

Figure 12. Acceleration response of horizontal vibration of car system with time delay of 2 ms. (A) Time-domain response; (B) Frequency response.

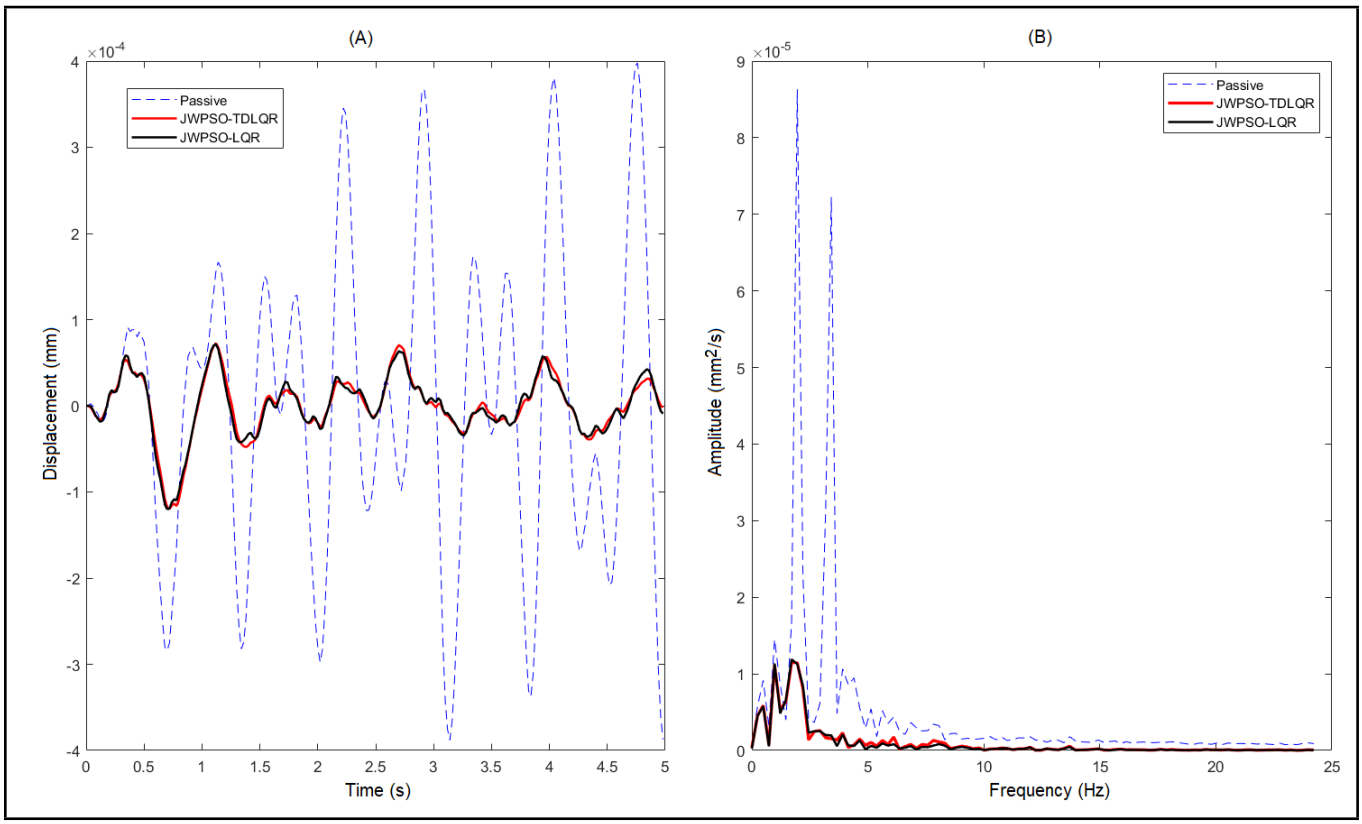

Figure 13. Displacement response of horizontal vibration of car system with time delay of 2 ms. (A) Time-domain response; (B) Frequency response.

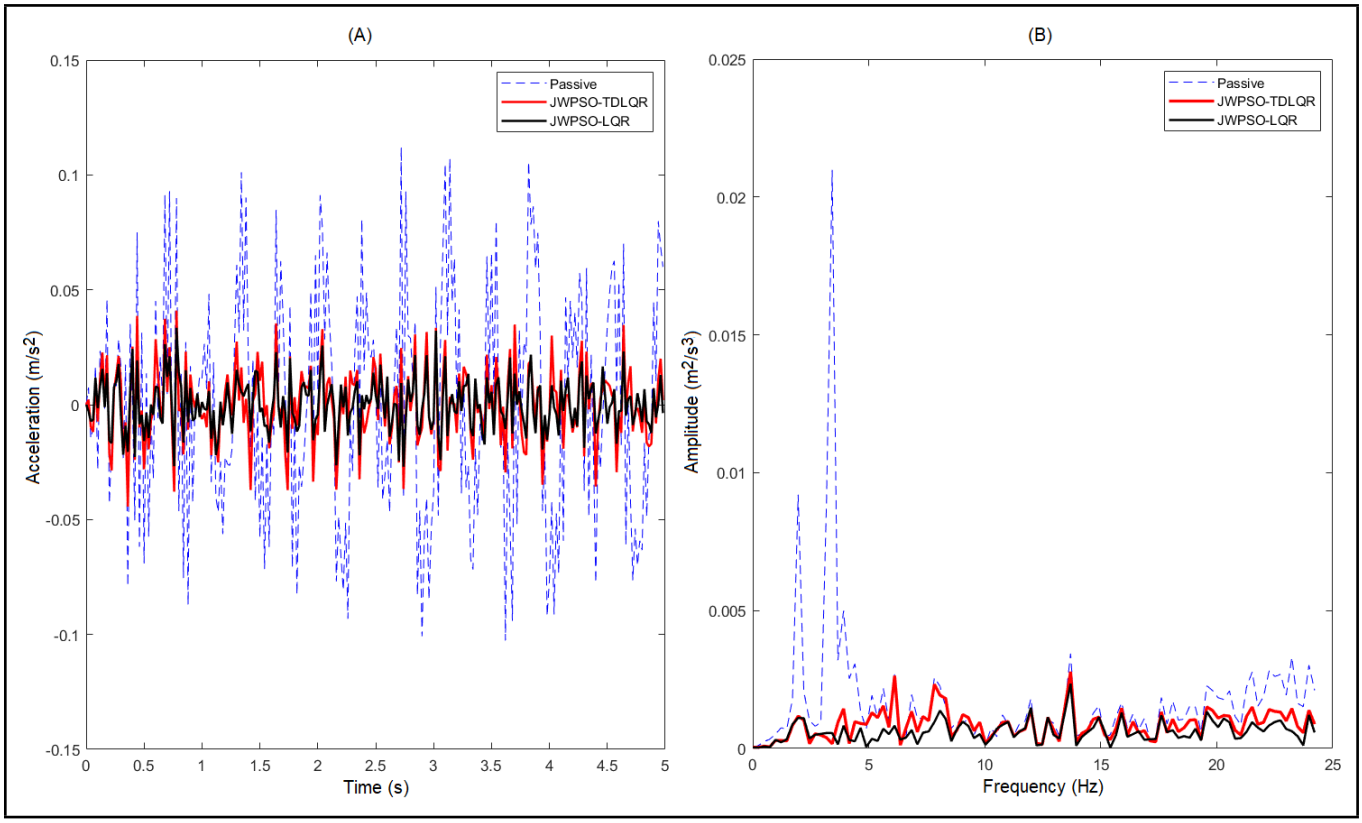

Figure 14. Acceleration response of horizontal vibration of car system with time delay of 5 ms. (A) Time-domain response; (B) Frequency response.

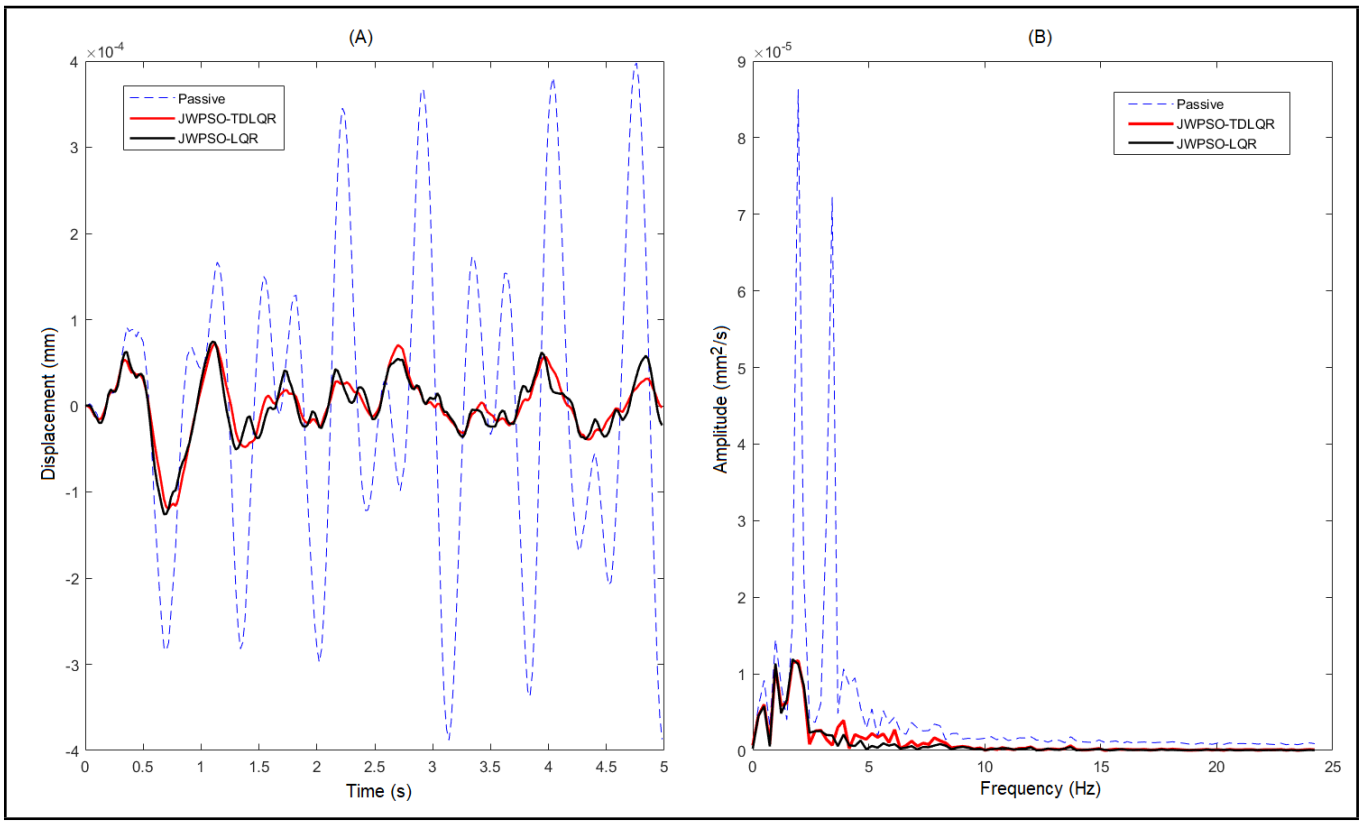

Figure 15. Displacement response of horizontal vibration of car system with time delay of 5 ms. (A) Time-domain response; (B) Frequency response.

Table 4. The typical numerical characteristics under control in light load situations.

Statement	Acceleration			Displacement		
	MAX (m/s^2)	RMS	FP	MAX (mm)	RMS	FP
Passive	0.1131	0.0457	0.0018	0.27	1.2e-4	5.9e-5
JWPSO-LQR	0.0361	0.0131	0.0003	0.08	3.0e-5	9.2e-6
JWPSO-TDLQR (2 ms)	0.0441	0.0157	0.0003	0.078	3.0e-5	9.4e-6
JWPSO-TDLQR (5 ms)	0.0460	0.0173	0.0003	0.08	3.1e-5	9.3e-6

Table 5. The typical numerical characteristics under control in heavy load situations.

Statement	Acceleration			Displacement		
	MAX (m/s^2)	RMS	FP	MAX (mm)	RMS	FP
Passive	0.1121	0.0482	0.0021	0.398	1.8e-4	8.6e-5
JWPSO-LQR	0.0335	0.0114	0.0003	0.073	3.5e-5	7.2e-5
JWPSO-TDLQR (2 ms)	0.0416	0.0143	0.0003	0.072	3.5e-5	7.2e-5
JWPSO-TDLQR (5 ms)	0.0410	0.0164	0.0003	0.075	3.7e-5	7.3e-5

Table 6. The typical numerical characteristics of the VDV value.

Statement	Light load	Heavy load
Passive	0.087	0.090
JWPSO-LQR	0.026	0.022
JWPSO-TDLQR (2 ms)	0.031	0.028
JWPSO-TDLQR (5 ms)	0.034	0.032

the ideal JWPSO-LQR for vibration response reduction under two kinds of time delays, and the difference of typical response characteristics is less than 5%, which proves the effectiveness and robustness of the JWPSO-LQR controller designed in this paper.

From the above simulation analysis, the JWPSO-LQR controller and JWPSO-TDLQR controller designed in this paper can effectively reduce the vibration acceleration and vibration displacement of the elevator in the time and frequency domains under different load cases.

The whole process of car operation is selected as the research object, and the vibration does VDV is used to detect passenger comfort.[31] VDV is defined as:

$$VDV = \left[\int_0^T a_w^4(t)dt\right]^{1/4}; \tag{31}$$

where T is the duration of the vibration signal and a_w^4 is the acceleration of the vibration signal after the weighting of the frequency meter. The VDV values of JWPSO-TDLQR and JWPSO-LQR were calculated under light load and heavy load conditions, respectively, as shown in Table 6.

As shown in Table 6, the VDV value of JWPSO-LQR decreases by 70% for the light load condition, 64% for the case of 2 ms time delay, and 61% for the case of 5 ms time delay compared to no control. At heavy load condition, the VDV value of JWPSO-LQR decreases by 76% compared with no control, and the VDV decreases by 69% for the case of 2 ms time delay and 64% for the case of 5 ms time delay. It shows that the designed controller can effectively reduce the horizontal vibration of the elevator and improve passenger comfort.

6.2. Control Effect of JWPSO-TDLQR, JWPSO-LQR, and GA-LQR Controller on Car Horizontal Vibration

To prove the superiority of the proposed controller, this paper uses the GA-LQR controller presented in Jia et al.[32] as the contrast object. It compares the car system's horizontal vibration acceleration and vibration displacement response in the same elevator model state.

Table 7. The typical numerical characteristics under the JWPSO-TDLQR, JWPSO-LQR, and GA-LQR.

Statement	Acceleration		Displacement	
	MAX (m/s^2)	RMS	MAX (mm)	RMS
Passive	0.1131	0.0457	0.27	1.2e-4
GA-LQR	0.0856	0.0323	0.21	4.5e-5
JWPSO-TDLQR	0.0460	0.0173	0.08	3.1e-5
JWPSO-LQR	0.0361	0.0131	0.08	3.0e-5

Table 8. The typical numerical characteristics under the 5 ms delay.

Statement	Acceleration		Displacement	
	MAX (m/s^2)	RMS	MAX (mm)	RMS
Passive	0.1131	0.0457	0.27	1.2e-4
LMI-H∞	0.0824	0.0293	0.21	8.5e-4
JWPSO-TDLQR	0.0460	0.0173	0.08	3.1e-5

The response comparison of horizontal vibration acceleration and displacement under the control of JWPSO-TDLQR, JWPSO-LQR, and GA-LQR is shown in Fig. 16, and the digital characteristics are shown in Table 7.

According to the response curve and the characteristics, compared with the situation of GA-LQR, the MAX and RMS of horizontal vibration acceleration controlled by JWPSO-TDLQR decreased by 46% and 58%, respectively, and the index of vibration displacement decreased by 47% and 59%. Compared with the situation of GA-LQR, the MAX and RMS of horizontal vibration acceleration controlled by JWPSO-LQR decreased by 62% and 62%, respectively, and the index of vibration displacement decreased by 31% and 33%. By comparing the control effect of JWPSO-TDLQR, JWPSO-LQR, and GA-LQR, it can be seen that the control effect of the proposed controller on the digital characteristics of the car vibration is more evident than the GA-LQR in the previous research, which verifies the superiority of the proposed controller.

6.3. Control Effect of JWPSO-TDLQR and LMI-H∞ Controller on Car Horizontal Vibration

To prove the superiority of the proposed controller, this paper uses the LMI-H∞ controller presented in Chang et al.[17] as the contrast object. It compares the car system's horizontal vibration acceleration and vibration displacement response in the same elevator model state.

The response comparison of horizontal vibration acceleration and displacement under the control of JWPSO-TDLQR and LMI-H∞ is shown in Fig. 17, and the digital characteristics are shown in Table 8.

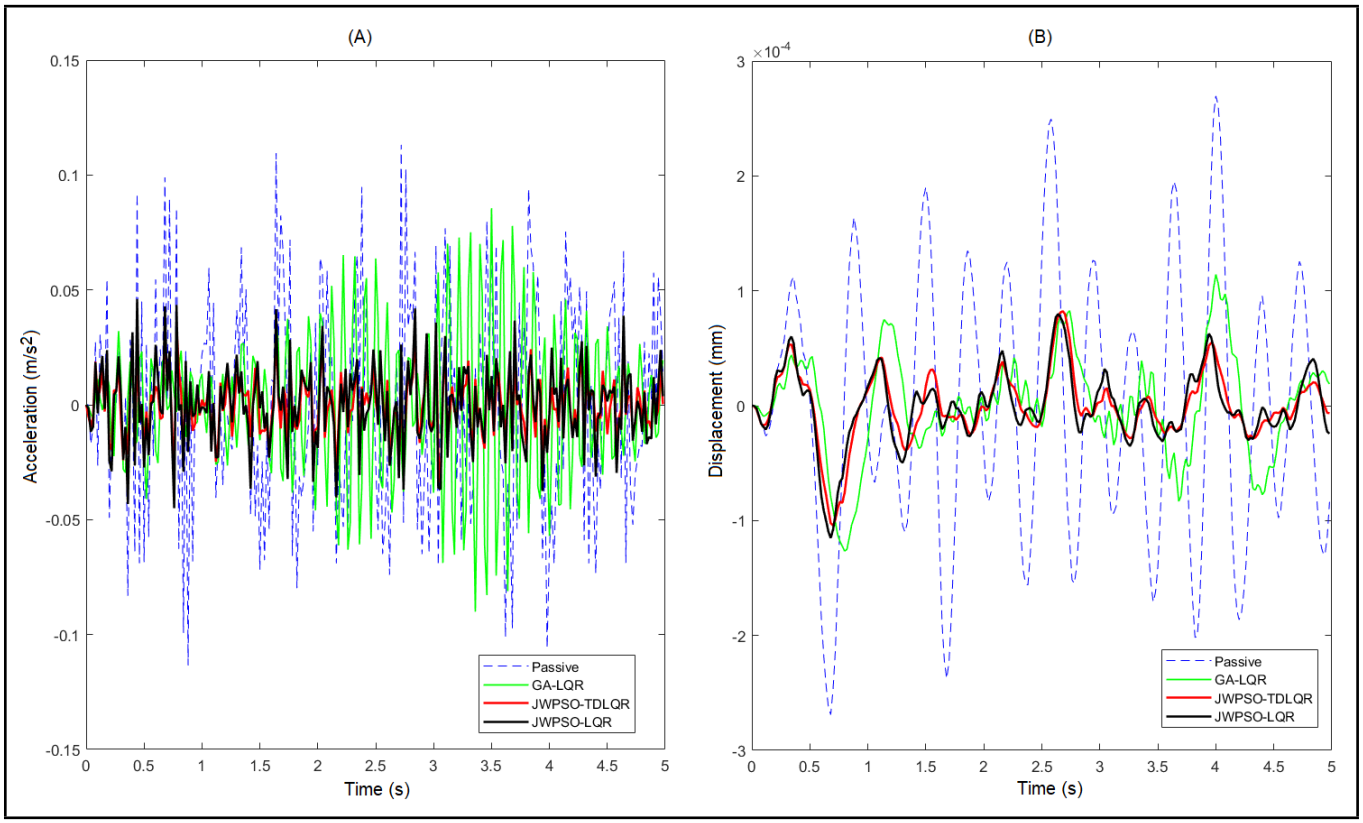

Figure 16. Vibration response of horizontal vibration of car system under the control of JWPSO-TDLQR and GA-LQR. (A) Time-domain response; (B) Time-domain response.

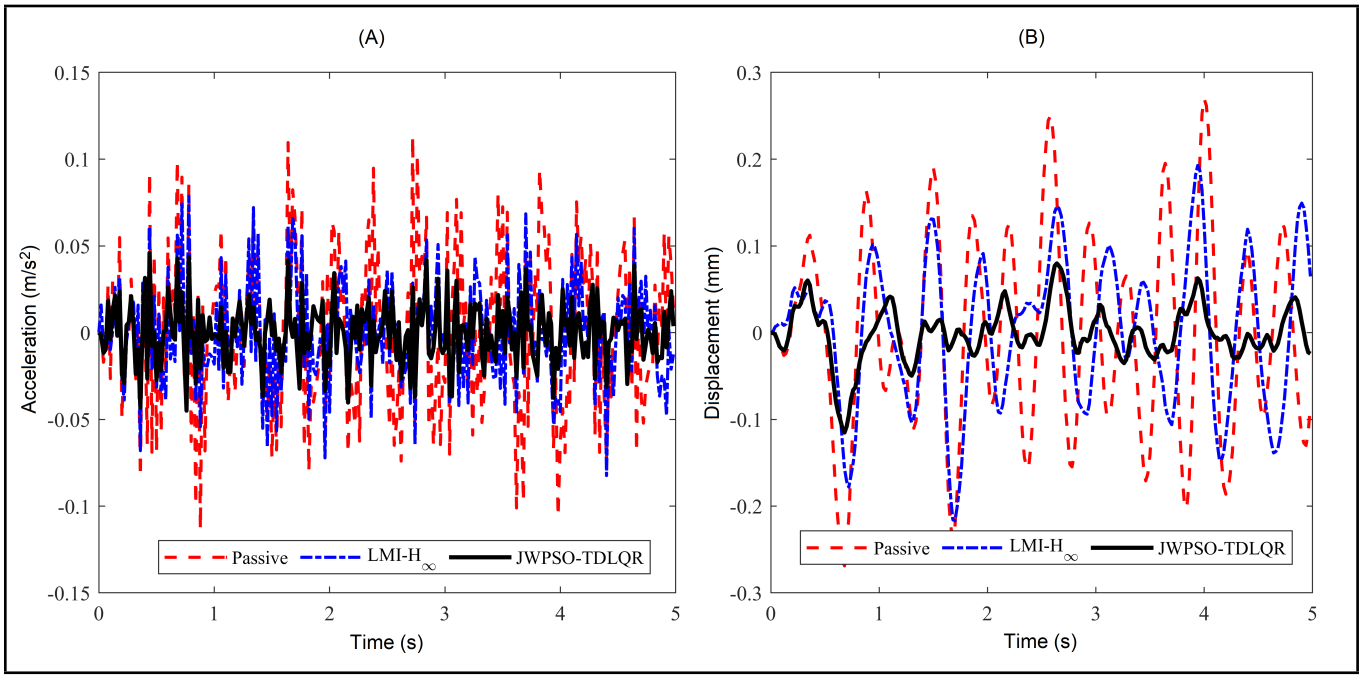

Figure 17. Vibration response of horizontal vibration of car system under the control of JWPSO-TDLQR and LMI-H∞. (A) Time-domain response; (B) Time-domain response.

According to the response curve and the characteristics, compared with the situation of LMI-H∞, the MAX and RMS of horizontal vibration acceleration controlled by JWPSO-TDLQR decreased by 41% and 49%, respectively, and the index of vibration displacement decreased by 82% and 74%. By comparing the control effect of JWPSO-TDLQR and LMI-H∞, it can be seen that the control effect of the proposed controller on the digital characteristics of the car vibration is more evident than the LMI-H∞ in the previous research, which verifies the superiority of the proposed controller.

Through the above simulation experiments, it can be seen that, when the JWPSO-TDLQR designed in this paper is used to reduce the horizontal vibration of the car, the proposed controller can effectively track the ideal state control effect when

the actuator delay is 2 ms and 5 ms. Moreover, compared with the GA-LQR controller and the LMI-H∞ controller proposed in the previous literature, the controller designed in this paper also has a better control effect. The robustness and control superiority of the proposed controller is verified, which provides a new method for elevator vibration reduction.

7. CONCLUSION AND FUTURE OUTLOOK

1. This study designed a new type of differential magnetic suspension active guide shoe based on the principle of the differential electromagnet magnetic suspension actuator. Compared with the traditional hydraulic active guide shoe, the active guide shoe has the advantages of no friction, no contact, and fast response. Compared with the unidirectional electromagnetic active guide shoe, the differential magnetic suspension actuator can realize two-way operation output the control force under the condition of only changing the size of the electric current.

2. The quadratic controller value function is designed based on the output weighting method, and the stability of the LQR controller is analyzed. Considering the particle swarm algorithm's optimization-seeking accuracy and convergence speed (PSO). Based on the basic particle swarm optimization (PSO) algorithm, proposed a Jumping inertia Weight Particle Swarm Optimization (JWPSO) algorithm, used the joint fitness function of optimization algorithm proved that JWPSO algorithm has better optimization effect than PSO algorithm. TDLQR is designed based on the dynamic model of car vibration considering the actuator time delay. The JWPSO algorithm is applied to adaptively seek the optimal TDLQR weight coefficient matrix to obtain the optimal weight coefficient matrix of the TDLQR controller.

3. In this paper, simulation experiments proved that the JWPSO-TDLQR could attenuate above 60% of the MAX and RMS of the horizontal vibration acceleration under different kinds of delay conditions. The results show that the control effect of the proposed controller can effectively track the control effect of ideal JWPSO-LQR, and the damping effect is better than GA-LQR and LMI-H∞, which verified the superiority of the control method, and has a critical reference significance for reducing the horizontal vibration of the high-speed elevator car and improving the ride comfort of the elevator.

4. The controllers designed in this paper are all under ideal conditions. During the operation of the elevator, the center of mass of the elevator car will change dynamically due to the change in the number of passengers. Therefore, to control the horizontal vibration of high-speed elevators more accurately during operation, it is necessary to explore further the effect of dynamic changes in load and load position on elevator vibration.

ACKNOWLEDGEMENTS

This research was funded by the Shandong Province Natural Science Foundation, China (GRANT NO. ZR2017MEE049) and the Key Research Development Project of Shandong Province (GRANT NO.2018GSF122004). The authors are grateful for the equipment support provided by Shandong FJZY Elevator Co., Ltd. The authors sincerely thank the editors and reviewers for their insights and comments to further improve the quality of the manuscript.

REFERENCES

[1] Crespo, R. S., Kaczmarczyk, S., Picton, P., and Su, H. Modelling and simulation of a stationary high-rise elevator system to predict the dynamic interactions between its components, *International Journal of Mechanical Sciences*, **137**, 24–45, (2018). https://doi.org/10.1016/j.ijmecsci.2018.01.011

[2] Mei, D. Q., Du, X. Q., and Chen, Z. Z. Vibration analysis of high-speed traction elevator based on guide roller-rail contact model, *Journal of Mechanical Engineering*, **45** (5), 264–270, (2009). https://doi.org/10.3901/JME.2009.05.264

[3] Zhang, R. J., Wang, C., Zhang, Q., and Liu, J. Response analysis of non-linear compound random vibration of a high-speed elevator, *Journal of Mechanical Science and Technology*, **33** (1), 51–63, (2019). https://doi.org/10.1007/s12206-018-1206-5

[4] Wang, C., Zhang, R. J., and Zhang, Q. Analysis of transverse vibration acceleration for a high-speed elevator with random parameter based on perturbation theory, *International Journal of Acoustics and Vibration*, **22** (2), 218–223, (2017). https://doi.org/10.20855/ijav.2017.22.2467

[5] Zhang, S. H., Zhang, R. J., He, Q., and Cong, D. S. The analysis of the structural parameters on dynamic characteristics of the guide rail-guide shoe-car coupling system, *Archive of Applied Mechanics*, **88** (11), 2071–2080, (2018). https://doi.org/10.1007/s00419-018-1437-z

[6] Knezevic, B. Z., Blanusa, B., and Marcetic, D. P. A synergistic method for vibration suppression of an elevator mechatronic system, *Journal of Sound and Vibration*, **406**, 29–50, (2017). https://doi.org/10.1016/j.jsv.2017.06.006

[7] Bao, J. H., Zhang, P., Zhu, C. M., et al. Vibration control of high-speed elevator hoisting systems based on tensioning devices, *Journal of Vibration and Shock* (in Chinese), **36** (14), 221–226, (2017). https://doi.org/10.13465/j.cnki.jvs.2017.14.035

[8] Ai, Y. Y., Wang, Z., and Li, L. X. Study on the active vibration control of high-speed traction-elevator, *Journal of Vibration and Shock* (in Chinese), **26** (6), 56–58, 78, (2007). https://doi.org/10.13465/j.cnki.jvs.2007.06.013

[9] Yu, H. Y., Zhang, X., and Dong, X. H. A novel adaptive control for elevator system with observer and parameter identification, *Proc. of the 2009 IEEE International Conference on Automation and Logistics*, Shenyang, China, (2009). https://doi.org/10.1109/ICAL.2009.5262848

[10] Kamel, M., Kandil, A., El-Ganaini, W. A., and Eissa, M. Active vibration control of a non-linear magnetic levitation system via Non-linear Saturation Controller (NSC), *Nonlinear Dynamics*, **77** (3), 605–619, (2014). https://doi.org/10.1007/s11071-014-1323-3

[11] Moazen, M., Sharifian, M. B. B., and Afshari, H. PID control of maglev guiding system for linear elevator, *Proc. of the 2012 IEEE 5th India International Conference on Power Electronics*, Delhi, INDIA, (2012). https://doi.org/10.1109/IICPE.2012.6450409

[12] Yu, D. M., Hao, M. L., and Liu, H. Fuzzy control of maglev guiding system in liner elevator based on feedback linearization, *Proc. of the 2011 IEEE 30th Chinese Control Conference*, 2899-2902, (2011).

[13] Song, C. S., Hu, Y. F., and Zhou, Z. D. Research on the control mechanism of differential active magnetic suspension vibration isolation system, *Journal of Vibration and Shock* (in Chinese), **29** (7), 24–27, 104, (2010). https://doi.org/10.13465/j.cnki.jvs.2010.07.018

[14] He, L., Li, Y., and Yang, J. Theory and experiment of passive-active hybrid vibration isolation mounts using electromagnetic actuator and air spring, *Acta Acoustics* (in Chinese), **38** (02), 241–249, (2013). https://doi.org/10.15949/j.cnki.0371-0025.2013.02.014

[15] Feng, Y. H., Zhang, J. W., and Zhao, Y. Modeling and robust control of horizontal vibrations for high-speed elevator, *Journal of Vibration and Control*, **15** (9),1375–1396, (2009). https://doi.org/10.1177/1077546308096102

[16] Feng, Y. H. and Zhang, J. W. The modeling and simulation of horizontal vibrations for high-speed elevator, *Journal Of Shanghai Jiaotong University*, **41** (4), 557–560, (2007).

[17] Chang, C.-C., Lin, C.-C., Su, W.-C., and Huang, Y.-P. H∞ Direct Output Feedback Control of High-Speed Elevator Systems, *Proc. of the ASME Pressure Vessels and Piping Conference*, 289–296, Baltimore, MD, USA, (2011). https://doi.org/10.1115/PVP2011-57814

[18] Chen, C., Zhang, R. J., Zhang, Q., and Liu, L. X. Mixed H2/H∞ guaranteed cost control for high-speed elevator active guide shoe with parametric uncertainties, *Mechanics & Industry*, **21** (5), 502, (2020). https://doi.org/10.1051/meca/2020044

[19] Chen, C., Zhang, R. J., and Zhang, Q. Finite frequency H∞ control for active guide shoe of high-speed elevator with actuator delay, *Mechanisms and Machine Science*, **105**, 644–652, (2021). https://doi.org/10.1007/978-3-030-75793-9_62

[20] Cao, S. X., He, Q., and Zhang, R. J. Robust control of high speed elevator transverse vibration based on LMI optimization, *Proc. of ICMMME 2019—4th International Conference on Manufacturing, Material and Metallurgical Engineering*, Chengdu, China, (2019). https://doi.org/10.1088/1757-899X/538/1/012032

[21] Santo, D. R., Balthazar, J. M., Tusset, A. M., Piccirilo, V., Brasil, R., and Silveira, M. On non-linear horizontal dynamics and vibrations control for high-speed elevators, *Journal of Vibration and Control*, **24** (5), 825–838, (2018). https://doi.org/10.1177/1077546316667324

[22] He, Q., Zhang, P., Cao, S. X., Zhang, R. J., and Zhang, Q. Intelligent control of horizontal vibration of high-speed elevator based on gas–liquid active guide shoes, *Mechanics & Industry*, **22** (2), (2021). https://doi.org/10.1051/meca/2020100

[23] Zhang, Q., Yang, Z., Wang, C., Yang, Y., and Zhang, R. Intelligent control of active shock absorber for high-speed elevator car, *Proc. of the Institution of Mechanical Engineers, Part C: Journal of Mechanical Engineering Science*, **233** (11), 3804–3815, (2019). https://doi.org/10.1177/0954406218810045

[24] Shi, Y. H. and Eberhart, R. C. A modified particle swarm optimizer, *Proc. of the IEEE Conference on Evolutionary Computation*, 69–73, Anchorage, USA, (1998).

[25] Kai, S., Fan, S., and Chiu, Y. Y. A decreasing inertia weight particle swarm optimizer, *Engineering Optimization*, **39** (2), 203–228, (2007). https://doi.org/10.1080/03052150601047362

[26] Li, M., Chen, H., Wang, X. D., Zhong, N., and Lu, S. An improved particle swarm optimization algorithm with adaptive inertia weights, *International Journal of Information Technology & Decision Making*, **18** (3), 833–866, (2019). https://doi.org/10.1142/S0219622019500147

[27] Das, R. R., Elumalai, V. K., Subramanian, R. G., and Kumar, K. V. A. Adaptive predator-prey optimization for tuning of infinite horizon LQR applied to vehicle suspension system, *Applied Soft Computing*, **72**, 518–526, (2018). https://doi.org/10.1016/j.asoc.2018.06.044

[28] Ma, L., Lu, C. W., Gu, Q. H., et al., Particle swarm optimization with search operator of improved pigeon-inspired algorithm, *Pattern Recognition and Artificial Intelligence* (in Chinese), **31** (10), 909–920, (2018). https://doi.org/10.16451/j.cnki.issn1003-6059.201810005

[29] Liu, D. H., Hu, X. Y., Zhao, Y. S., and Cui, Y. Particle swarm optimization method based on dynamic sub-swarms with entropy weight, *Journal Of Xidian University* (in Chinese), **45** (6), 69–74, (2018). https://doi.org/10.3969/j.issn.1001-2400.2018.06.012

[30] Xia, B. H. and Shi, X. Horizontal vibrations of high-speed elevator with guide rail excitation, *Machinery Manufacturing & Automation* (in Chinese), **41** (5),161–165, (2012). https://doi.org/10.19344/j.cnki.issn1671-5276.2012.05.053

[31] British Standard Guide, BS 6841: Measurement and evaluation of human exposure to whole-body mechanical vibration and repeated shock, BSI, London, (1987).

[32] Jia, T. C., He, Q., and Zhang, R. J. Study on linear quadratic regulator of high-speed elevator car horizontal vibration based on genetic algorithm optimization, *Mechanisms and Machine Science*, **105**, 607–615, (2021). https://doi.org/10.1007/978-3-030-75793-9_58

APPENDIX

$$\mathbf{A}=\begin{bmatrix}\mathbf{A}_{11} & \mathbf{A}_{12} & \mathbf{A}_{13}\\ \mathbf{A}_{21} & \mathbf{A}_{22} & \mathbf{A}_{23}\\ \mathbf{A}_{31} & \mathbf{A}_{32} & \mathbf{A}_{33}\end{bmatrix};$$

$$\mathbf{A}_{11}=\begin{bmatrix}0 & 0 & 1 & 0\\ 0 & 0 & 0 & 1\\ \frac{-4k_s}{m_c} & \frac{2k_s(L_1-L_2)}{m_c} & \frac{-4c_s}{m_c} & \frac{2c_s(L_1-L_2)}{m_c}\\ \frac{2k_s(L_1-L_2)}{I_c} & \frac{-2k_s(L_1^2+L_2^2)}{I_c} & \frac{2c_s(L_1-L_2)}{I_c} & \frac{-2c_s(L_1^2+L_2^2)}{I_c}\end{bmatrix};$$

$$\mathbf{A}_{12}=\begin{bmatrix}0 & 0 & 0 & 0\\ 0 & 0 & 0 & 0\\ \frac{k_s}{m_c} & \frac{k_s}{m_c} & \frac{k_s}{m_c} & \frac{k_s}{m_c}\\ \frac{-k_sL_1}{I_c} & \frac{-k_sL_1}{I_c} & \frac{k_sL_2}{I_c} & \frac{k_sL_2}{I_c}\end{bmatrix};$$

$$\mathbf{A}_{13}=\begin{bmatrix}0 & 0 & 0 & 0\\ 0 & 0 & 0 & 0\\ \frac{c_s}{m_c} & \frac{c_s}{m_c} & \frac{c_s}{m_c} & \frac{c_s}{m_c}\\ \frac{-c_sL_1}{I_c} & \frac{-c_sL_1}{I_c} & \frac{c_sL_2}{I_c} & \frac{c_sL_2}{I_c}\end{bmatrix};$$

$$\mathbf{A}_{21}=\mathbf{A}_{22}=\begin{bmatrix}0 & 0 & 0 & 0\\ 0 & 0 & 0 & 0\\ 0 & 0 & 0 & 0\\ 0 & 0 & 0 & 0\end{bmatrix};$$

$$\mathbf{A}_{23}=\begin{bmatrix}1 & 0 & 0 & 0\\ 0 & 1 & 0 & 0\\ 0 & 0 & 1 & 0\\ 0 & 0 & 0 & 1\end{bmatrix};$$

$$\mathbf{A}_{31}=\begin{bmatrix}\frac{k_s}{m_r} & \frac{-k_sL_1}{m_r} & \frac{c_s}{m_r} & \frac{-c_sL_1}{m_r}\\ \frac{k_s}{m_r} & \frac{-k_sL_1}{m_r} & \frac{c_s}{m_r} & \frac{-c_sL_1}{m_r}\\ \frac{k_s}{m_r} & \frac{k_sL_2}{m_r} & \frac{c_s}{m_r} & \frac{c_sL_2}{m_r}\\ \frac{k_s}{m_r} & \frac{k_sL_2}{m_r} & \frac{c_s}{m_r} & \frac{c_sL_2}{m_r}\end{bmatrix};$$

$$\mathbf{A}_{32}=\begin{bmatrix}\frac{-(k_s+k_r)}{m_r} & 0 & 0 & 0\\ 0 & \frac{-(k_s+k_r)}{m_r} & 0 & 0\\ 0 & 0 & \frac{-(k_s+k_r)}{m_r} & 0\\ 0 & 0 & 0 & \frac{-(k_s+k_r)}{m_r}\end{bmatrix};$$

$$\mathbf{A}_{33}=\begin{bmatrix}\frac{-c_r}{m_r} & 0 & 0 & 0\\ 0 & \frac{-c_r}{m_r} & 0 & 0\\ 0 & 0 & \frac{-c_r}{m_r} & 0\\ 0 & 0 & 0 & \frac{-c_r}{m_r}\end{bmatrix};$$

$$\mathbf{B}=\begin{bmatrix}\mathbf{B}_1\\ \mathbf{B}_2\end{bmatrix};$$

$$\mathbf{B}_1=\begin{bmatrix}0 & 0 & 0 & 0\\ 0 & 0 & 0 & 0\\ \frac{1}{m_c} & \frac{1}{m_c} & \frac{1}{m_c} & \frac{1}{m_c}\\ \frac{-L_1}{I_c} & \frac{-L_1}{I_c} & \frac{L_2}{I_c} & \frac{L_2}{I_c}\\ 0 & 0 & 0 & 0\\ 0 & 0 & 0 & 0\end{bmatrix};$$

$$\mathbf{B}_2=\begin{bmatrix}0 & 0 & 0 & 0\\ 0 & 0 & 0 & 0\\ \frac{-1}{m_r} & 0 & 0 & 0\\ 0 & \frac{-1}{m_r} & 0 & 0\\ 0 & 0 & \frac{-1}{m_r} & 0\\ 0 & 0 & 0 & \frac{-1}{m_r}\end{bmatrix};$$

$$\mathbf{R}=\begin{bmatrix}\mathbf{R}_1\\ \mathbf{R}_2\end{bmatrix};$$

$$\mathbf{R}_1=\mathbf{0}_{6\times 8};$$

$$\mathbf{R}_2=\begin{bmatrix}0 & 0 & 0 & 0 & 0 & 0 & 0 & 0\\ 0 & 0 & 0 & 0 & 0 & 0 & 0 & 0\\ \frac{k_r}{m_r} & 0 & 0 & 0 & 0 & 0 & 0 & 0\\ 0 & \frac{k_r}{m_r} & 0 & 0 & 0 & 0 & 0 & 0\\ 0 & 0 & \frac{k_r}{m_r} & 0 & 0 & 0 & 0 & 0\\ 0 & 0 & 0 & \frac{k_r}{m_r} & 0 & 0 & 0 & 0\end{bmatrix};$$

$$\mathbf{C}=\begin{bmatrix}\mathbf{C}_{11} & \mathbf{C}_{12} & \mathbf{C}_{13}\\ \mathbf{C}_{21} & \mathbf{C}_{22} & \mathbf{C}_{23}\end{bmatrix};$$

$$\mathbf{C}_{11}=\begin{bmatrix}1 & 0 & 0 & 0\\ 0 & 1 & 0 & 0\\ 0 & 0 & 0 & 0\\ 0 & 0 & 0 & 0\end{bmatrix};$$

$$\mathbf{C}_{12}=\begin{bmatrix}0 & 0 & 0 & 0\\ 0 & 0 & 0 & 0\\ 1 & 0 & 0 & 0\\ 0 & 1 & 0 & 0\end{bmatrix};$$

$$\mathbf{C}_{13}=\mathbf{0}_{4\times 4};$$

$$\mathbf{C}_{21}=\begin{bmatrix}0 & 0 & 1 & 0\\ 0 & 0 & 0 & 1\\ \frac{-4k_s}{m_c} & \frac{2k_s(L_1-L_2)}{m_c} & \frac{-4c_s}{m_c} & \frac{2c_s(L_1-L_2)}{m_c}\\ \frac{2k_s(L_1-L_2)}{I_c} & \frac{-2k_s(L_1^2+L_2^2)}{I_c} & \frac{2c_s(L_1-L_2)}{I_c} & \frac{-2c_s(L_1^2+L_2^2)}{I_c}\end{bmatrix};$$

$$\mathbf{C}_{22}=\begin{bmatrix}0 & 0 & 0 & 0\\ 0 & 0 & 0 & 0\\ \frac{k_s}{m_c} & \frac{k_s}{m_c} & \frac{k_s}{m_c} & \frac{k_s}{m_c}\\ \frac{-k_sL_1}{I_c} & \frac{-k_sL_1}{I_c} & \frac{k_sL_2}{I_c} & \frac{k_sL_2}{I_c}\end{bmatrix};$$

$$\mathbf{C}_{23}=\begin{bmatrix}0 & 0 & 0 & 0\\ 0 & 0 & 0 & 0\\ \frac{c_s}{m_c} & \frac{c_s}{m_c} & \frac{c_s}{m_c} & \frac{c_s}{m_c}\\ \frac{-c_sL_1}{I_c} & \frac{-c_sL_1}{I_c} & \frac{c_sL_2}{I_c} & \frac{c_sL_2}{I_c}\end{bmatrix};$$

$$\mathbf{D}=\begin{bmatrix}0 & 0 & 0 & 0\\ 0 & 0 & 0 & 0\\ 0 & 0 & 0 & 0\\ 0 & 0 & 0 & 0\\ 0 & 0 & 0 & 0\\ 0 & 0 & 0 & 0\\ \frac{1}{m_c} & \frac{1}{m_c} & \frac{1}{m_c} & \frac{1}{m_c}\\ \frac{-L_1}{I_c} & \frac{-L_1}{I_c} & \frac{L_2}{I_c} & \frac{L_2}{I_c}\end{bmatrix}.$$